CHAPTER 4

Results & Discussion

4. Results and discussion

This chapter details and describes the results of the scientific investigations to achieve the doctoral research's primary goal, i.e., to design and develop a photobioreactor capable of mass-scale microalgae cultivation and production of microalgae biomass for biofuel production. This chapter is subdivided into three subchapters according to the primary objectives of this research. The contents of the subchapters are synopsized below.

4A. To design and develop a photobioreactor (PBR) for mass-scale microalgae cultivation.

This chapter describes the design philosophies of the three microalgae culture systems being developed. The chapter also illustrates the advantages and limitations of the developed microalgae culture systems. Finally, the chapter demonstrates the findings of the scientific experimentations and analysis carried out in the developed microalgae culture systems.

4B. To optimize the culture conditions and improve the biomass and lipid productivity.

The stacked try automated modular photobioreactor (STAMP) was the chosen microalgae photobioreactor capable of mass-scale microalgae cultivation at a commercial scale. The STAMP's performance or biomass productivity was thereby improved by optimizing the culture conditions like light intensity, light duration, light wavelength, airflow rate, and nitrogen content using Face Centered Central Composite Design approach of Response Surface Methodology. The optimization is detailed in this chapter.

4C. To analyze the algal biomass and biofuel properties produced from the microalgae cultured in the developed PBR.

This chapter details the analytical findings to characterize the biomass and biofuels obtained from the microalgae culture systems developed during the current investigation. The calorific value, ash content, lipid content, lipid characterization using GC-MS, biofuel production estimation using ^{1}H-NMR spectroscopy, oil density, acid value, and carbon residue are characterized and compared with the global standards in this chapter.

CHAPTER 4A

To design and develop a photobioreactor (PBR) for mass-scale microalgae cultivation.

4A. To design and develop a photobioreactor (PBR) for mass-scale microalgae cultivation.

This chapter details the design philosophies incorporated for developing the microalgae culture system suitable for mass-scale microalgae cultivation. The chapter also details the findings of the experiments carried out during the development process. Finally, the experimental validations of the developed Stacked Tray Automated Modular Photobioreactor (STAMP), considered suitable for mass-scale microalgae cultivation, are illustrated in this chapter.

4A.1 Design philosophy of the Internally Illuminated Stirred Light Column Photobioreactor (IISLCP)

The open ponds are the most successful microalgae culture systems, contributing over 90% of commercial microalgae biomass production globally [1]. This is because open ponds are easy and economical to construct and operate compared to other microalgae cultivation systems [2, 3]. However, various limitations like low biomass productivity & density, less control over the operational parameters, contamination problems, and, most importantly, the need for large open areas having suitable environmental conditions (dry with low rainfall) limit the widescale implementation of these open microalgae culture systems [3, 4]. The other types of systems are the photobioreactor system, which are closed systems with high contamination resistance, much higher productivity compared to open systems, compact design compared to open systems, and high control over operational parameters [5-7]. However, closed photobioreactors are costly to build, operate, and maintain, resulting in the limitation of these systems.

To overcome the abovementioned limitations, the IISLCP photobioreactor design was conceptualized to be built using low-cost materials to reduce the capital cost. The photobioreactor systems used widely at present, like the tubular photobioreactor, the plate type photobioreactor, the vertical column photobioreactors, etc., mostly use transparent materials to let light penetrate inside the system. The transparent materials must be durable enough to withstand exterior weather conditions [8] and have a large surface-to-volume ratio to increase the surface area for light collection, increasing the material requirement and cost. The IISCLP design eliminates the need for costly transparent material and can be constructed using comparatively low-cost opaque materials. The need for transparent material was eliminated by designing the IISCLP to be shaped like a giant cylindrical water tank, which can be built using materials like PVC, plastic, etc. The

illumination was provided by inserting LED strips into the culture media. With the advancement of semiconductor technology, the cost of LEDs has drastically reduced in the past decades [9]. The cost of photovoltaic panels has also decreased drastically, and their efficiencies have increased significantly, making it feasible and economical to harness solar energy and power LEDs [9]. The IISCLP was conceptualized to exploit this advancement in semiconductor technologies and develop a low-cost, highly compact photobioreactor system.

Another critical design aspect incorporated in the IISCLP was a rotating axel-based LED support system, as shown in Figure 4A.1(a & b). The concept of this design was to achieve uniform light distribution in each corner of the PBR and also achieve proper mixing of the culture media, which is essential for efficient microalgal growth. As the central axel rotates, the flat spokes in the bottom of the LED support ring force the microalgae culture upwards, thus preventing the microalgae from settling to the bottom of the culture tank. The developed system was tested, and further developments are discussed in the following section.

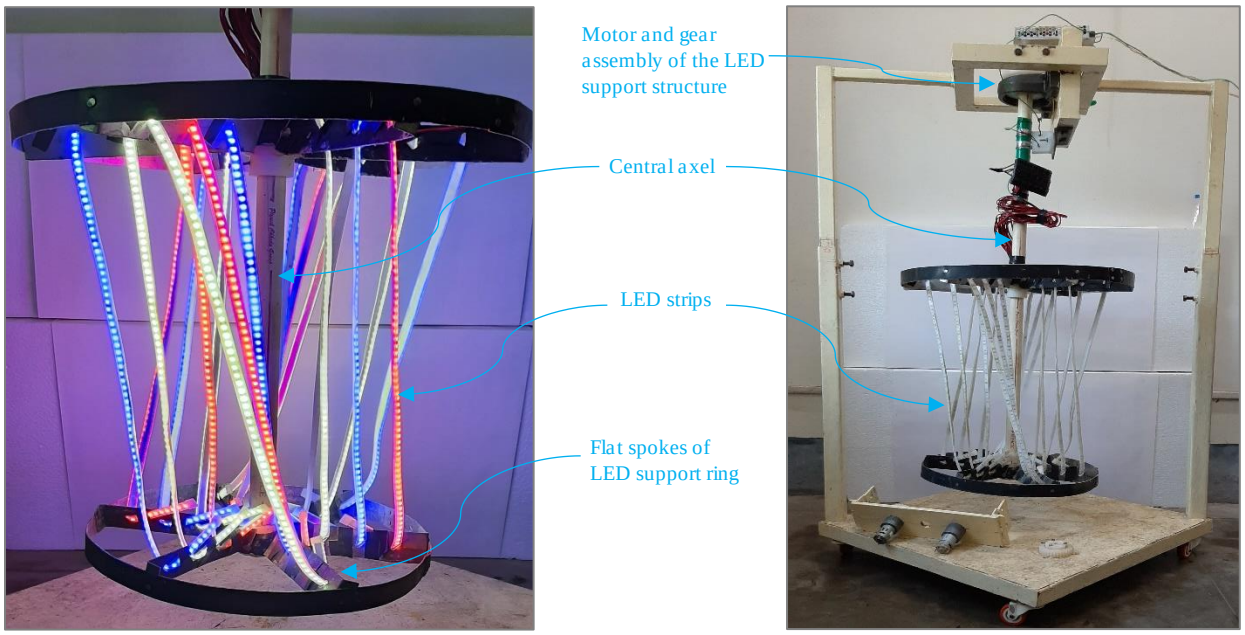

Figure 4A.1 (a): The internal illumination system of the IISCLP system consisting the LED strips, support rings and the central axel, in an illuminated state. **(b):** The internal illumination system of the IISCLP system along with the support structure and gear and motor assembly.

4A.1.1. Microalgae culture analysis in the IISCLP system

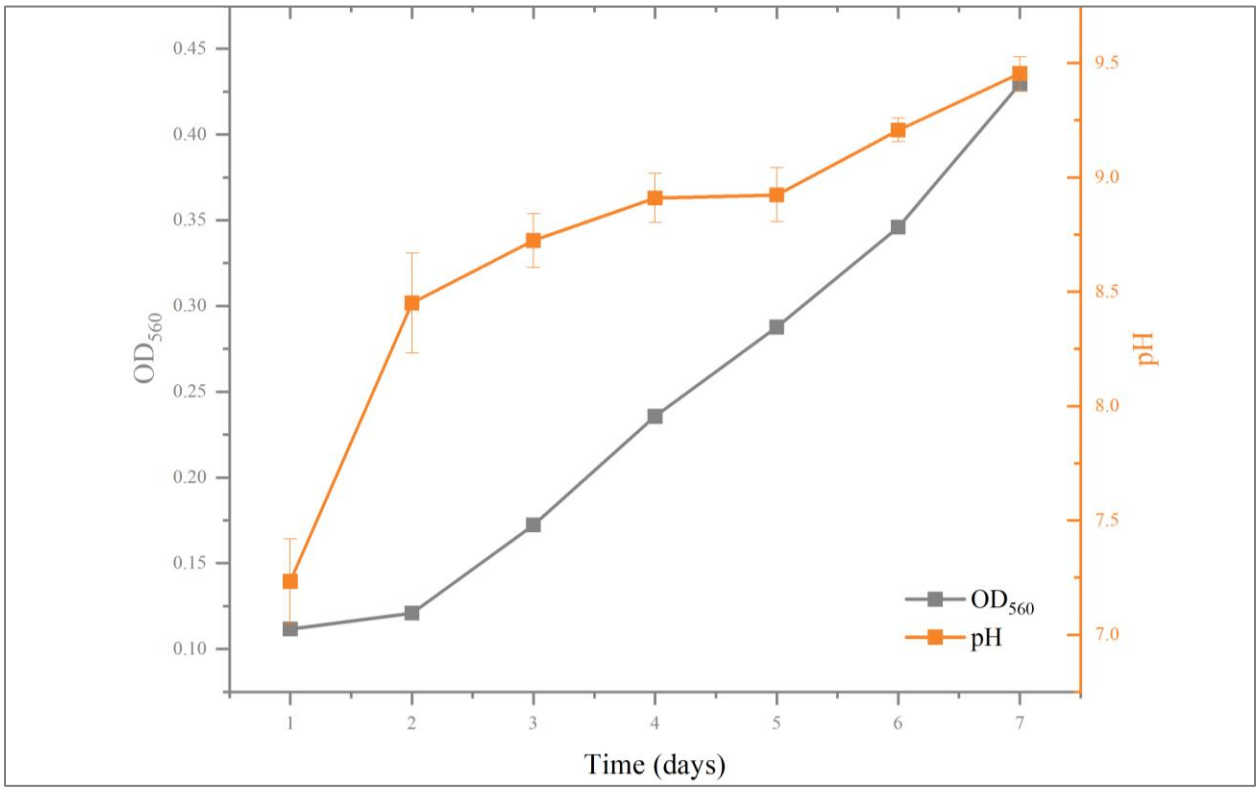

Figure 4A.2: Microalgae growth and pH of the microalgae culture, grown in the IISCLP system monitored for 7 days.

Growth of the *Chlorella homosphaera* microalgae species cultured using BG11 media in the developed IISCLP system was monitored by measuring the absorbance at 560 nm (OD_{560}). 100 L BG11 media containing 1.5 g/L sodium nitrate ($NaNO_3$) used as nitrogen source was inoculated with *C. homosphaera* microalgae inoculum to achieve a starting culture having initial OD_{560} of around 0.11±0.002. The culture was illuminated with a 16:8 hours light/dark cycle and the illumination intensity to 1600 Lux. The rotation of the central shaft with the LEDs was maintained at 20 rpm. After seven days of culture, the microalgae growth measured by OD_{560} was found to be 0.43, giving a specific growth rate of 0.224 day^{-1}. The specific growth rate is significantly higher, over twofold higher, compared to the growth rate of 0.1 day^{-1} obtained by Guo et al. [10], cultivating *Chlorella pyrenoidosa* microalgae species using blue LED illumination. The specific growth rate obtained is also much higher compared to the growth rate achieved in the most successful commercial microalgae cultivation system, i.e., open raceway pond system ranging between 0.154-0.197 day^{-1} as reported by Zhu et al. [11].

However, the specific growth rate is significantly lower compared to 1.26 day^{-1} reported by Ziganshina et al. [12], growing *Chlorella sorokiniana* microalgae species in modified Bold's basal medium (BBM) with NH_4^+ as a nitrogen source. The productivity and efficiency of IISCLP were planned to be improved by optimizing parameters like light intensity, light wavelength, light duration, nitrogen and carbon content, mixing rate, etc. One of the factors hampering the productivity in the IISCLP was the rise in the pH of the solution, almost reaching 9.5 at the end of 7 days, as seen in Figure 4A.2. Addition of CO_2 by bubbling air supplemented with CO_2 into the culture will help in maintaining the pH as well as boost the productivity as demonstrated by Ziganshina et al. [12], was planned to be incorporated in the further studies.

However, due to technical issues like degradation of the Teflon gears, regular failure of the motors used, and problems with the contact brushes used for conducting electricity to power the LEDs in the rotating structure, the design raised concern regarding its success in widescale implementation for cost-effective commercial microalgae production. Thus, the IISCLP design was not explored further, and the research focused on the next version of the photobioreactor, i.e., the Internally Illuminated Airlift Photobioreactor (IIAP). Apart from the mechanical issues, which could be fixed with detailed engineering of the parts, the major problem of IISCLP design, which raised concerns about its success, was biofouling. Details of the biofouling issue are discussed in the later section of this chapter.

4A.2 Design philosophy of the Internally Illuminated Airlift Photobioreactor (IIAP)

The Internally Illuminated Airlift Photobioreactor (IIAP) system design emphasized the system's cost reduction by using comparatively low-cost opaque material for the system design and focused on LED-based internal illumination. The IIAP design considered fewer moving parts to reduce wear and tear and improve the system's longevity. The IIAP system design was influenced by one of the microalgae culture systems designed and developed in the GreenTec laboratory at the Federal University of Rio de Janeiro (UFRJ), Brazil. The system designed at UFRJ is an internally illuminated photobioreactor system made of opaque material, as shown in Figure 4A.3(a). The internal illumination was provided using a bundle of Plastic Optical Fiber Cables (POFCs), Figure 4A.3(c), distributed uniformly inside the developed photobioreactor, Figure 4A.3(d). Sunlight was collected using a Fresnel lens at the top of the building fitted with a solar tracker to focus sunlight to an IR filter and through it to the POFC cables, Figure 4A.3(b).

The system had several limitations such as the Fresnel lens can harness only direct sunlight and is almost ineffective in utilizing diffused solar radiation, the use of POFC cables is quite costly as they cannot be branched, and thus all the cables that are used to illuminate the culture inside the PBR have to travel from the PBR to the point of collection, i.e., to the place where the Fresnel lens is placed. Lastly, the diffusion of the light inside the PBR was challenging because light exited through the tip of the POFC, Figure 4A.3(c).

(a) **(b)** **(c)** **(d)**

Figure 4A.3 (a): The POFC based photobioreactor developed and placed at the terrace of GreenTec Laboratory, UFRJ, Brazil **(b):** The Fresnel lens, IR filter and the POFC cables assembly with the solar tracker system **(c):** The illuminated POFC cables dispersing light from its tips **(d):** The POFC assembly with its support structure of the developed photobioreactor.

The IIAP overcomes the aforementioned limitations by replacing the POFC-based illumination with LED-based illumination. The Fresnel lens and IR filter assembly mounted on the solar tracker gets replaced with PV panels. In this arrangement, the solar energy harnessed by the PV can be transmitted to a longer distance where the IIAP is placed at a comparatively lower cost using electric cables. Additionally, the PV panels can efficiently harness both direct and diffused solar radiation increasing efficiently.

Thus, the IIAP was developed by submerging LED strips vertically into the culture media, placed systematically to achieve uniform illumination inside the IIAP system. Air was bubbled from the bottom of the reactor using diffuser tubes placed at the bottom. As the air bubble rises, CO_2 in the air stream dissolves into the culture medium, providing the essential carbon source the microalgae needs to grow. The upward-moving air bubbles also prevented the microalgae from settling to the

bottom and kept the microalgae cells afloat, improving their growth. The air diffuser was designed so that the air bubbles moved close to the surface of the vertical LED strips, thereby carrying away any microalgae cells that try to attach to the LED strips, preventing biofouling.

Additionally, the IIAP was fitted with an electronic control system to control the culture parameters of the IIAP system. The initial control system developed controls the light intensity, light duration, and airflow duration. The developed IIAP system was initially tested by microalgae culture experiments. The system was planned to be upgraded with other sensors, like pH sensors and control CO_2 supplement in the airstream for improved efficiency, in the later stage of development.

4A.2.1 Temperature control of the IIAP system

One of the essential parameters was the temperature control of the culture media. As the LED strips are submerged in the culture media, the heat emitted by the LED strips, although minimal, builds up and increases the temperature of the culture media. In the current investigation, the culture temperature was controlled to keep it in the range favorable for the growth of the cultured microalgae species *Chlorella homosphaera*. The temperature control was achieved using the LED intensity and the air stream. The LED strips acted as the heat source. Thus, when it was needed to increase the temperature, the LEDs were powered to their full potential, and when it was required to cool down, the LED power was reduced, and the airflow carried away the heat, reducing the temperature. For certain microalgae species or locations where further cooling of the culture medium might be required, an additional cooling system can be installed to cool down the air stream. However, in the present scenario, for the culture of *C. homosphaera*, the ambient temperature of Tezpur, Assam, which ranges between 25-35 ℃, was suitable. Thus, additional cooling of the airstream was not required.

Figure 4A.4 depicts the temperature control achieved using the developed control system for the IIAP. The temperature control was achieved using ON-OFF control logic and was set to dim the LED intensity once the temperature surpassed the set value of 32 ℃. The light was set for 18:6 light/dark interval. Initially, the temperature gradually increased from the ambient temperature of about 30 ℃ to the set value of 32 ℃ and was maintained at that level. The control system was turned OFF for a certain duration to test the temperature control system's efficacy. It can be seen

that the temperature of the culture spiked above the set value and reached almost 34 ℃. The control system was turned back again, and the temperature could remain stable and remained in the range of 32 ℃. During the off periods, the temperature falls to the ambient temperature of 30 ℃, which is in the favorable range of *C. homosphaera* cultivation. Thus, no additional heating was needed.

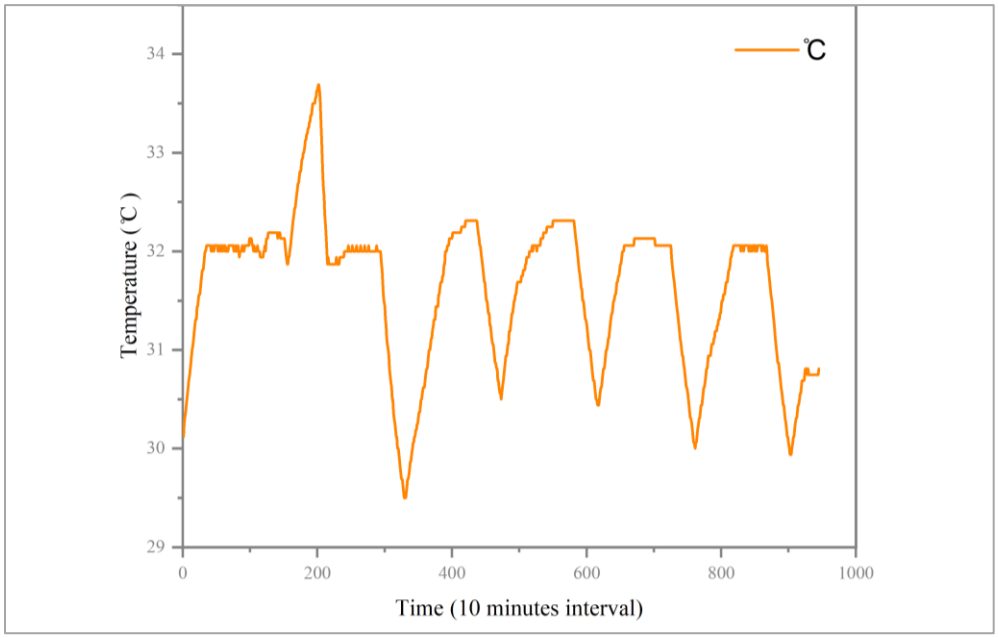

Figure 4A.4: Temperature control achieved using Arduino based control system in the IIAP system.

Thus, overall, the temperature control achieved with the developed control system was successful. The temperature control was planned to be improvised to use PD or PID-based control with further development of the IIAP. However, due to one major issue, the issue of biofouling, the system seemed to be unfavorable for mass-scale culture. Thus, further research on the system was suspended and moved on to the next system, tackling the issue of biofouling.

4A.3. The issue with biofouling in a photobioreactor

Biofouling is microalgae growth on a solid surface, forming a thick layer, thereby blocking light from passing through it. In the developed IISCLP and IIAP systems, microalgae started growing on the LED strips and blocked the light from the LEDs from passing to the microalgae culture. As a result, the LED strips had to be cleaned every two to three days apart. Figure 4A.5 shows the damage caused to the LED strips after repeated cleaning of the accumulated microalgae on the surface of the LED strips. Various measures were implemented to prevent biofouling of the LED

strips in both the IISCLP and IIAP systems, like the rotational speed of the lighting arrangement was increased in the IISCLP system, and the airflow rate of the IIAP system was increased. However, none was adequate to prevent biofouling of the LED strips.

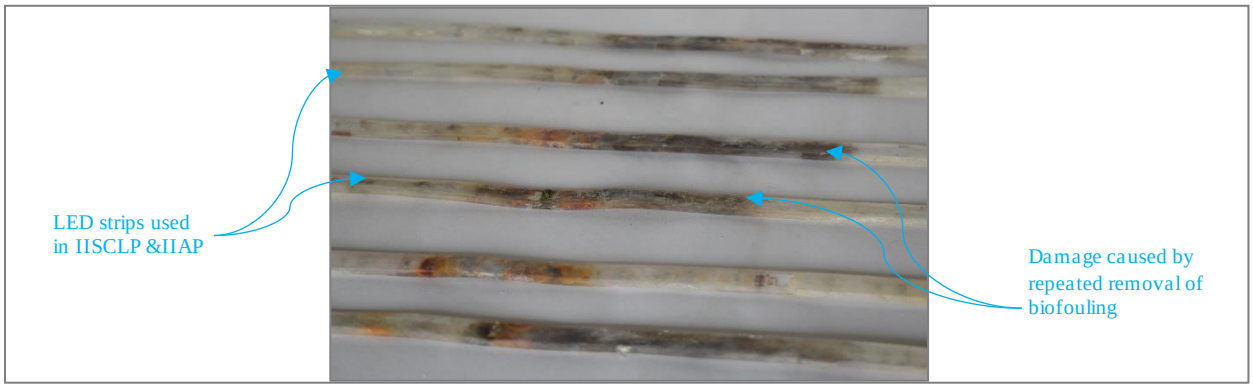

Figure 4A.5: Effect of biofouling on the LED strips used in the IISCLP and IIAP systems

Biofouling is a severe issue in photobioreactors, reducing biomass productivity and thereby necessitating regular cleaning and maintenance of the system, increasing the operational and maintenance cost and ultimately leading to an increase in the price of the produced microalgae biomass. Arbiba et al. [13] reported biofouling to be a significant issue of tubular photobioreactors, as shown in Figure 4A.6 (a), causing them to shut down the microalgae culture experiments conducted in the tubular photobioreactors. Similar issues caused by biofouling were also reported by Li et al. [14] in an airlift flat panel type photobioreactor, as shown in Figure 4A.6 (b), growing *Scenedesmus obliquus* microalgae strain. Biofouling not only decreases the productivity in a photobioreactor, it also causes other deteriorating effects on the microalgae culture like changes in cell pigmentation and contamination by invasive microorganisms, etc., as reported by Zeriouh et al. [15], necessitating the shutdown of the culture system.

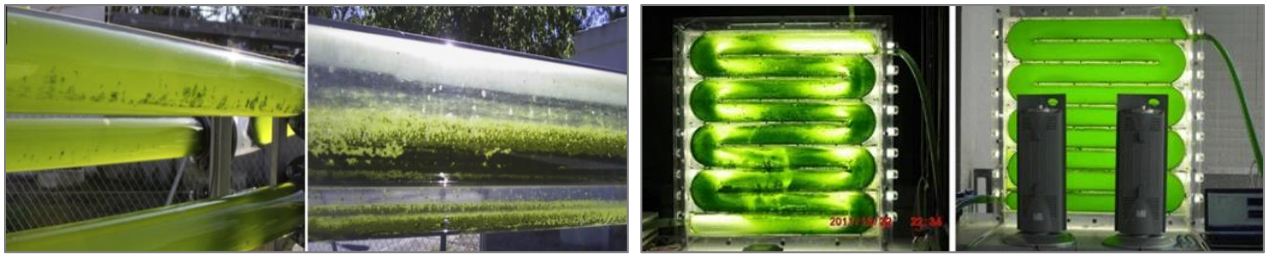

(a) (b)

Figure 4A.6 (a): Biofouling in tubular photobioreactor as reported by Arbiba et al. **(b):** Biofouling in flat plate air lift photobioreactor system reported by Li et al.

Researchers have adopted various preventive measures like increasing the flow velocity of microalgae culture to prevent microalgae from sticking to the surface [14], developing novel surface coating materials to prevent microalgae from sticking to the surface [15], etc. still the issue of biofouling could not be solved. It remains the major limitation of photobioreactor systems. Nguyen et al. [16] have ascertained biofouling as the most significant limitation of closed photobioreactor systems.

Thus, to develop a photobioreactor system capable of mass-scale microalgae culture, the bioreactor design should be able to prevent biofouling or be immune to biofouling. The Stacked Tray Automated Modular Photobioreactor (STAMP) system was designed and developed, with one of the primary goals being to solve the issue of biofouling.

4A.4 Design philosophy of the Stacked Tray Automated Modular Photobioreactor (STAMP)

The Stacked Tray Automated Modular Photobioreactor (STAMP) was designed from scratch to tackle biofouling. To achieve that goal, the design philosophy of the systems affected by biofouling and the ones unaffected by biofouling were studied in detail. Detailed studies revealed that almost all the closed photobioreactor systems, irrespective of their shape and size, like the tubular PBR, vertical column air lift PBR, flat plate PBR, and internally illuminated PBR, to name a few, almost all have the similarity that a solid transparent surface separates the microalgae culture and the light source. The microalgae culture is in direct contact with the surface, as shown in the schematic of Figure 4A.7. Microalgae tends to move toward the light source due to a phenomenon known as phototaxis [17, 18], causing them to move toward the solid transparent barrier and gradually sticking to it, which eventually leads to biofouling.

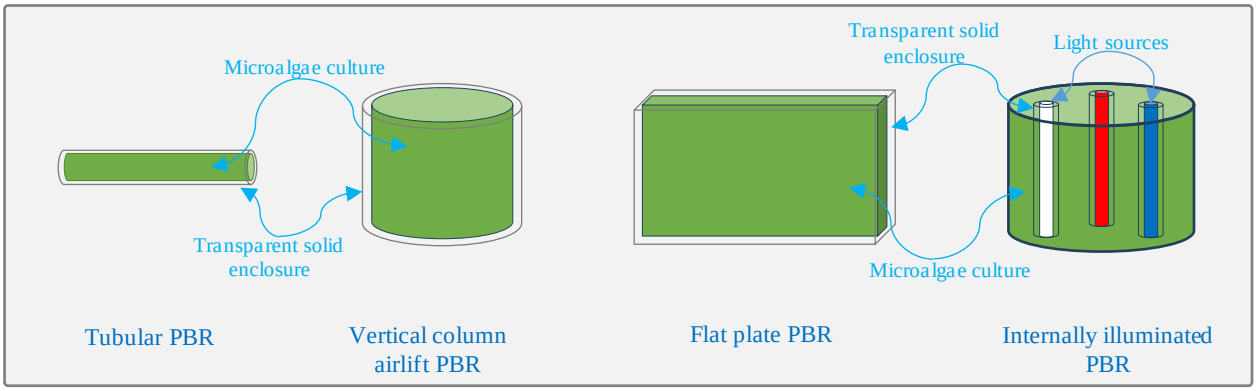

Figure 4A.7: Schematic representation of different types of photobioreactors commonly used for microalgae cultivation.

On the contrary, in the most successful microalgae cultivation systems, the open pond systems, the issue of biofouling is insignificant, as the microalgae culture and the light source are separated by a fluidic layer, i.e., air, and thus microalgae cannot stick to it and hence the light path always remains clear. Exploiting this phenomenon and coupled with the state-of-the-art semiconductor technology, the STAMP is designed and fabricated.

As illustrated in Figure 4A.8, the STAMP consists of microalgae culture trays stacked one above another, and each tray is illuminated using LED illumination. The air gap between the microalgae culture tray (MCT) and the LED panel prevents the microalgae from directly contacting the LED panel and, thus, prevents biofouling. Additionally, the air gap also helps to carry away the heat generated by the LEDs from the microalgae culture, which is minimal but has the potential to increase the temperature of the culture media if it accumulates, as seen in the case of the IIAP system.

The MCTs are made shallow for efficient light penetration. They are stacked one above another to compact the system and have more microalgae cultured per unit area compared to open raceway ponds. The stacked arrangement also helps in the circulation of the microalgae culture, where the microalgae are pumped from the bottommost MCT to the topmost MCT. The culture flows in the narrow channels created in the MCTs and exits the MCT to fall to the MCT placed below it. Likewise, the culture gradually descends back to the bottommost MCT. From the bottommost MCT, the culture flows to the raiser mixer unit, which is kept aerated to supply the microalgae culture with the necessary CO_2. The aerated culture is then pumped back to the topmost MCT, and the cycle continues.

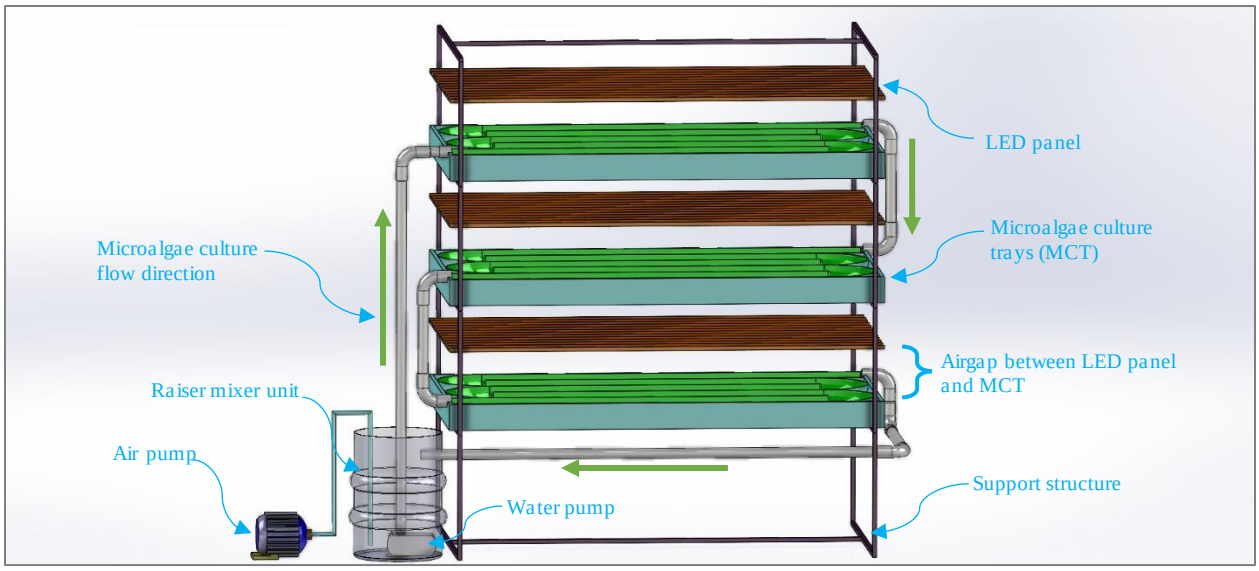

Figure 4A.8: Schematic view of the Stacked tray automated modular photobioreactor (STAMP) system.

The developed STAMP system, consisting of two MCTs having a net volume of 65 L, was initially tested by cultivating *C. homosphaera* microalgae in BG11 culture media. The initial test results are illustrated in the following sections. Following the successful initial trials, the STAMP system parameters were optimized using the Response Surface Methodology (RSM) described in the following chapter.

4A.4.1 Growth analysis of *Chlorella homosphaera* microalgae species in the developed STAMP system

Microalgae culture experiments were conducted in the developed STAMP to validate the system by culturing *C. homosphaera* microalgae species in BG11 culture media containing 1.5 gL^{-1} of sodium nitrate ($NaNO_3$) as the nitrogen source. Cool-while LED illumination was used for the initial trial and powered with 100% intensity, consuming 23.1 W power for illumination and with 16:8 light/dark mode. The air and water circulation were maintained during the light phase of the culture, i.e., for 16 hours per day. The water pump consumed 16 W power, and the air pump consumed 3W power. Initially, CO_2 from a CO_2 cylinder was used to supplement the air, but this was later stopped due to certain technical issues. Figure 4A.9 shows the growth of the microalgae measured by its OD_{560}.

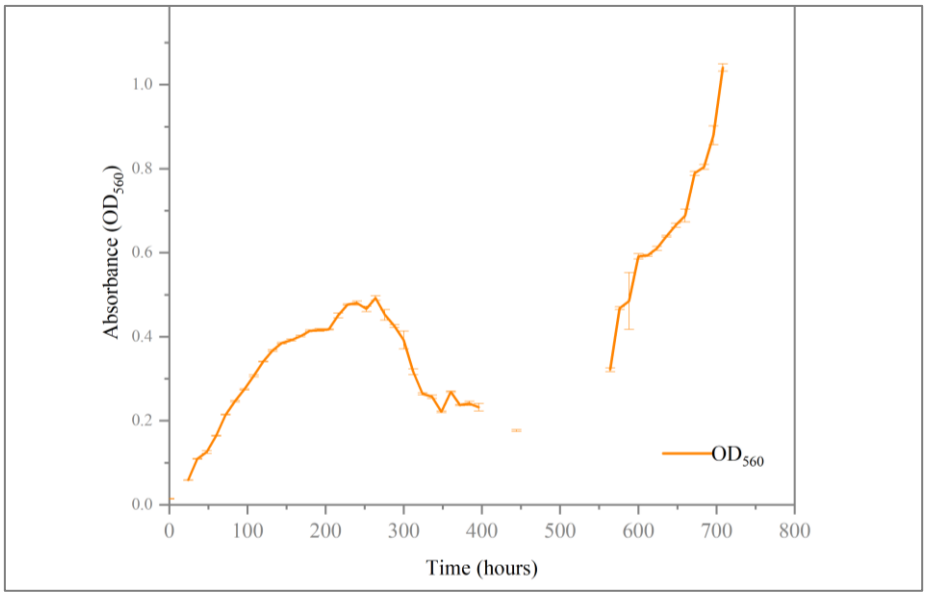

Figure 4A.9: Growth analysis of C. homosphaera microalgae species grown in the STAMP system

As seen in Figure 4A.9, the microalgae growth started at OD_{560} of 0.05, and the growth progressed pretty well for the initial ten days; however, the growth began to decline rapidly after that. The culture was stopped, and after a detailed investigation, the problem was found to be caused by the faulty pH measurements, which supplied access CO_2 to the culture media, making the culture media acidic. After rectifying the error and resuming the system, the culture bounced back and performed exceptionally well, as seen in the second half of the graph. The biomass productivity of 0.22 $gL^{-1}day^{-1}$ was achieved during the second cultivation phase. The biomass productivity achieved in the initial trial was better than that of widely used open raceway ponds, which ranges near 0.12 $gL^{-1}day^{-1}$ as reported by Sharma et al. [19] culturing *Chlorella minutissima* in a 1500 L open raceway pond. The comparatively better productivity can be owing to the better illumination provided in the STAMP system. However, the productivity was far lower compared to a well-established tubular PBR system reporting to achieve productivity of 0.5 $gL^{-1}day^{-1}$ by Tan et al. [20] culturing *Chlorella pyrenoidosa* using anaerobic food processing wastewater in a pilot-scale tubular photobioreactor system. The high growth rate achieved by Tan et al. can be attributed to a well-established culture routine and the availability of carbon sources. The performance of the STAMP will be improved further with the optimization of the culture parameters described in the following chapter.

4A.4.2 Evaluation of biofouling in the STAMP system

One of the primary design considerations of the STAMP system was biofouling prevention. Biofouling affects microalgae growth by forming an opaque film that blocks the light path and prevents it from reaching the microalgae culture. Thus, the growth of microalgae on the LED surface was evaluated to evaluate biofouling in the STAMP system. To estimate the microalgae growth on the LED surface, three glass slides were fixed on the LED panel's surface, and the glass slides' transmissivity was evaluated for the entire visible light spectrum, i.e., 400-800 nm wavelength, for one month at a seven-day interval. Figure 4A.10 shows the transmissivity readings of the glass slides. It can be seen that the transmissivity remained well above 97% for the entire duration of the one-month experiment. The slight variations ±1% can be owing to instrumental error, which can be considered negligible. This shows that even after one month of culture in the STAMP system, the LED surface remained clear of any microalgal growth, and thus, STAMP is almost immune to biofouling. Any biofouling on the side and bottom of the culture channel does not affect the system's performance as it does not come in the light path, which could block the light from entering the microalgae culture.

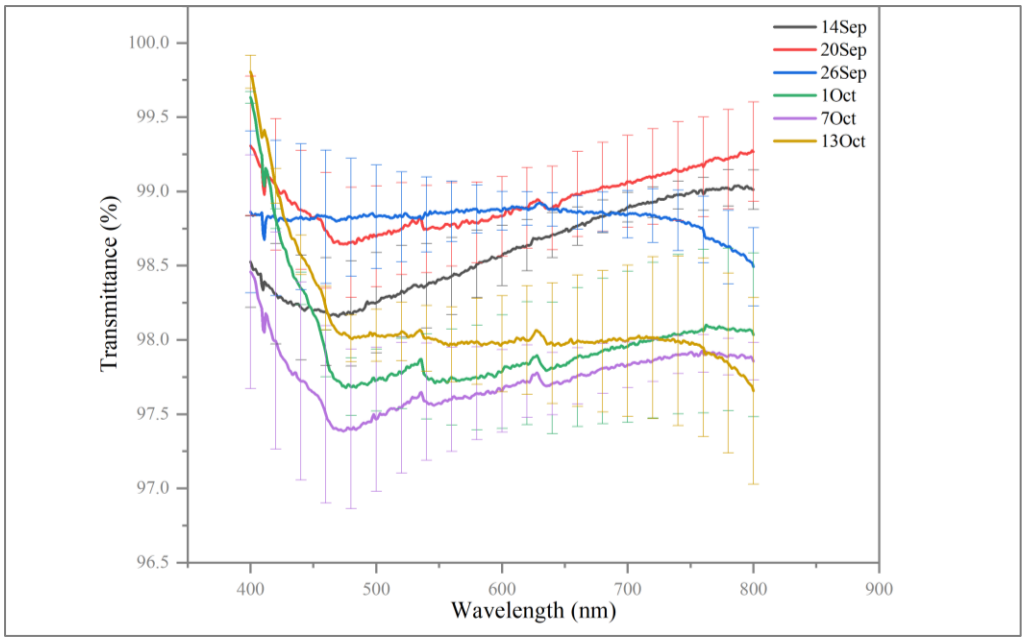

Figure 4A.10: Measurement of transmissivity of the glass slides placed on the surface of the LED panels facing the microalgae culture in the STAMP system.

4A.4.3 Temperature control in the developed STAMP system

The temperature of the culture media plays a significant role in microalgal growth, as microalgae are highly sensitive to changes in temperature. Thus, if the temperature of the culture media in the STAMP gets high due to the heat emitted by the LED panels, additional temperature control mechanisms must be installed. To evaluate the effect of temperature on the STAMP caused by the LED panels, the temperature in the culture media was monitored using temperature sensors submerged in the culture media, and the LEDs were turned on to their full potential, i.e., 23.1W power and with 16:8 light/day cycle. Figure 4A.11 illustrates the temperature profile variation caused by the STAMP system's LED illumination. As the LEDs are turned ON, the temperature increases gradually, and the temperature begins to drop as the LEDs are turned OFF. This implies that the LEDs affect the temperature of the STAMP system and that a cooling fan or other cooling mechanism might need to be installed in a larger-scale STAMP system. However, the temperature variation is negligible, i.e., just a 0.9 ℃ increase in 16 hours of illumination, which is in the tolerance range of *C. homosphaera* microalgae species currently cultured in the STAMP. Thus, no additional temperature control system is required for the current system.

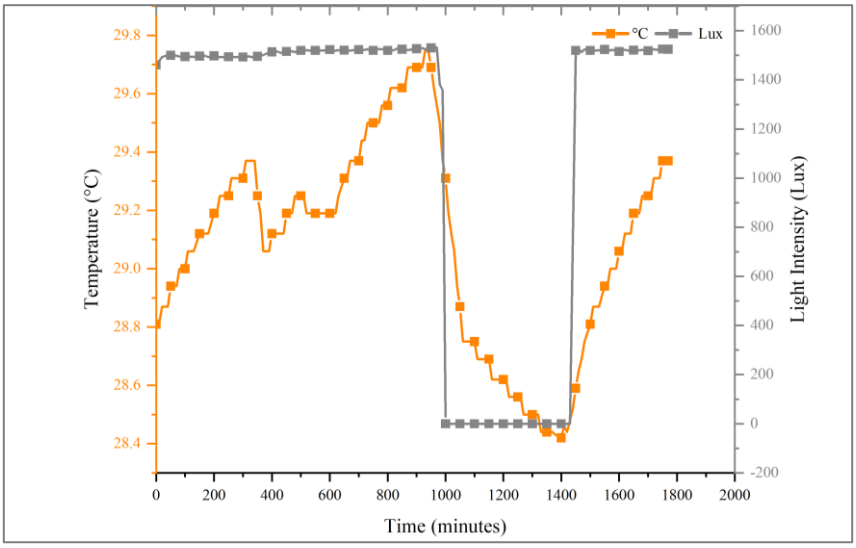

Figure 4A.11: Temperature variation caused by the LED illumination in the developed STAMP system.

4A.5 Summary

A microalgae culture system immune to biofouling was developed, and preliminary testing results were quite positive. Further design optimizations are needed to improve the system's productivity and make it suitable for commercial-scale microalgae cultivation.

References

[1] Schade, S. and T. Meier, *A comparative analysis of the environmental impacts of cultivating microalgae in different production systems and climatic zones: a systematic review and meta-analysis.* Algal research, 2019. **40**: p. 101485. DOI: https://doi.org/10.1016/j.algal.2019.101485.

[2] Costa, J.A.V., et al., *Open pond systems for microalgal culture*, in *Biofuels from algae*. 2019, Elsevier. p. 199-223.

[3] Borowitzka, M.A. and N.R. Moheimani, *Open pond culture systems*, in *Algae for biofuels and energy*. 2012, Springer. p. 133-152.

[4] Narala, R.R., et al., *Comparison of microalgae cultivation in photobioreactor, open raceway pond, and a two-stage hybrid system.* Frontiers in Energy Research, 2016. **4**: p. 29. DOI: https://doi.org/10.3389/fenrg.2016.00029.

[5] Assunção, J. and F.X. Malcata, *Enclosed "non-conventional" photobioreactors for microalga production: A review.* Algal research, 2020. **52**: p. 102107. DOI: https://doi.org/10.1016/j.algal.2020.102107.

[6] Chang, J.-S., et al., *Photobioreactors*, in *Current developments in biotechnology and bioengineering*. 2017, Elsevier. p. 313-352.

[7] Koller, M., *Design of closed photobioreactors for algal cultivation*, in *Algal Biorefineries: Products and Refinery Design*, A. Prokop, R.K. Bajpai, and M.E. Zappi, Editors. 2015, Springer, Cham. p. 133-186.

[8] Sero, E.T., et al., *Biophotonics for improving algal photobioreactor performance: A review.* International Journal of Energy Research, 2020. **44**(7): p. 5071-5092. DOI: https://doi.org/10.1002/er.5059.

[9] Kavlak, G., J. McNerney, and J.E. Trancik, *Evaluating the causes of cost reduction in photovoltaic modules.* Energy policy, 2018. **123**: p. 700-710. DOI: https://doi.org/10.1016/j.enpol.2018.08.015.

[10] Guo, H. and Z. Fang. *Effect of light quality on the cultivation of Chlorella pyrenoidosa*. in *E3S Web of Conferences*. 2020. EDP Sciences.

[11] Zhu, B., et al., *Large-scale cultivation of Spirulina for biological CO2 mitigation in open raceway ponds using purified CO2 from a coal chemical flue gas.* Frontiers in bioengineering and biotechnology, 2020. **7**: p. 441. DOI: https://doi.org/10.3389/fbioe.2019.00441.

[12] Ziganshina, E.E., S.S. Bulynina, and A.M. Ziganshin, *Growth characteristics of Chlorella sorokiniana in a photobioreactor during the utilization of different forms of nitrogen at various temperatures.* Plants, 2022. **11**(8): p. 1086. DOI: https://doi.org/10.3390/plants11081086.

[13] Arbib, Z., et al., *Long term outdoor operation of a tubular airlift pilot photobioreactor and a high rate algal pond as tertiary treatment of urban wastewater.* Ecological engineering, 2013. **52**: p. 143-153. DOI: https://doi.org/10.1016/j.ecoleng.2012.12.089.

[14] Li, J., et al., *Design and characterization of a scalable airlift flat panel photobioreactor for microalgae cultivation.* Journal of applied phycology, 2015. **27**: p. 75-86. DOI: https://doi.org/10.1007/s10811-014-0335-1.

[15] Zeriouh, O., et al., *Biofouling in photobioreactors for marine microalgae.* Critical reviews in biotechnology, 2017. **37**(8): p. 1006-1023. DOI: https://doi.org/10.1080/07388551.2017.1299681.

[16] Nguyen, L.N., et al., *Microalgae-based carbon capture and utilization: A critical review on current system developments and biomass utilization.* Critical Reviews in Environmental Science and Technology, 2023. **53**(2): p. 216-238. DOI: https://doi.org/10.1080/10643389.2022.2047141.

[17] Arrieta, J., et al., *Phototaxis beyond turning: persistent accumulation and response acclimation of the microalga Chlamydomonas reinhardtii*. Scientific reports, 2017. **7**(1): p. 3447. DOI: https://doi.org/10.1038/s41598-017-03618-8.

[18] Kreis, C.T., et al., *Adhesion of Chlamydomonas microalgae to surfaces is switchable by light.* Nature Physics, 2018. **14**(1): p. 45-49. DOI: https://doi.org/10.1038/nphys4258.

[19] Sharma, A.K., et al., *Production of a sustainable fuel from microalgae Chlorella minutissima grown in a 1500 L open raceway ponds.* Biomass and Bioenergy, 2021. **149**: p. 106073. DOI: https://doi.org/10.1016/j.biombioe.2021.106073.

[20] Tan, X.-B., et al., *Nutrients recycling and biomass production from Chlorella pyrenoidosa culture using anaerobic food processing wastewater in a pilot-scale tubular photobioreactor.* Chemosphere, 2021. **270**: p. 129459. DOI: https://doi.org/10.1016/j.chemosphere.2020.129459.

CHAPTER 4B

To optimize the culture conditions and improve the biomass and lipid productivity.

4B. To optimize the culture conditions and improve the biomass and lipid productivity.

The chapter demonstrates the methodology used to choose the LEDs for the RSM-based optimization of the performance parameters of the STAMP system. Then, the optimization of the operating parameters of the developed STAMP system using Face Centered Central Composite Design (FCCCD) approach of the statistical tool called response surface methodology (RSM) to obtain maximum biomass and lipid productivity of *Chlorella homosphaera* microalgae species are described. The operating parameters optimized in the current study are light wavelength, light intensity, light duration, nitrogen content, and airflow.

4B.1.1 Choosing LEDs for optimization of microalgae growth.

Six LED strips of different colors/wavelengths available commercially, cool white, warm white, pink, blue, red, and green color were procured. However, only four microalgae culture experimental setups were developed due to financial constraints. Thus, to choose four colors for the initial experimentations, the wavelength of the LEDs was investigated using a ThorLab Compact CCD Spectrometer (Model CCS200/M). The wave spectrums of the six LEDs are presented in Figure 4B.1(a-f).

Amongst all six available LEDs, the blue and red LEDs were first chosen to be investigated as various users have reported these LEDs to perform well for microalgae cultivation [1-5]. Mooij et al. [6] have supported the prevailing agreement that blue and red LEDs are optimal for microalgae cultivation owing to the corresponding peaks in the algal absorption spectrum. Wilhelm et al. [7] have reported that under blue illumination, *Chlorella fusca* microalgae species exhibited bigger cell sizes, thinner cell walls, and higher rates of photosynthesis. Kim et al. [1] found that Nannochloropsis gaditana grew better under red illumination and enhanced lipid accumulation while using red illumination for its cultivation. Thus, red and blue LEDs were primarily selected for the current investigation to be tested for STAMP.

Amongst the two white LEDs, it can be seen that the irradiance of both the cool-white and warm-white LEDs is spread across the entire visible spectrum, ranging from about 400nm to 780nm. The cool-white LED has a sharper irradiance peak in the blueish region (400-500 nm) compared to the warm-white LED, as seen in Figure 4B.1 a & b, respectively. Thus, among the two, cool-white was chosen to be investigated initially hoping for better performance as blue light promotes cell growth and enlargement [1, 7]. The warm white was kept to be investigated in the later stages. Of

the remaining two LEDs, i.e., the green and pink LED, the pink LED was selected for the current investigation owing to the two prominent peaks in the red and blue color region of its wave spectrum, as seen in Figure 4B.1 (c).

Additionally, Ritchie et al. [8] reported the pink LED has a clear blue peak at about 450 nm and a broad red peak from about 520 to 760 nm. It is currently used as a growth light for aquaponics and hydroponics cultivation and is also advantageous for microalgae cultivation. Various researchers reported that green LED induces stress in microalgae species [9] and is, thus, kept for investigation in the later stages.

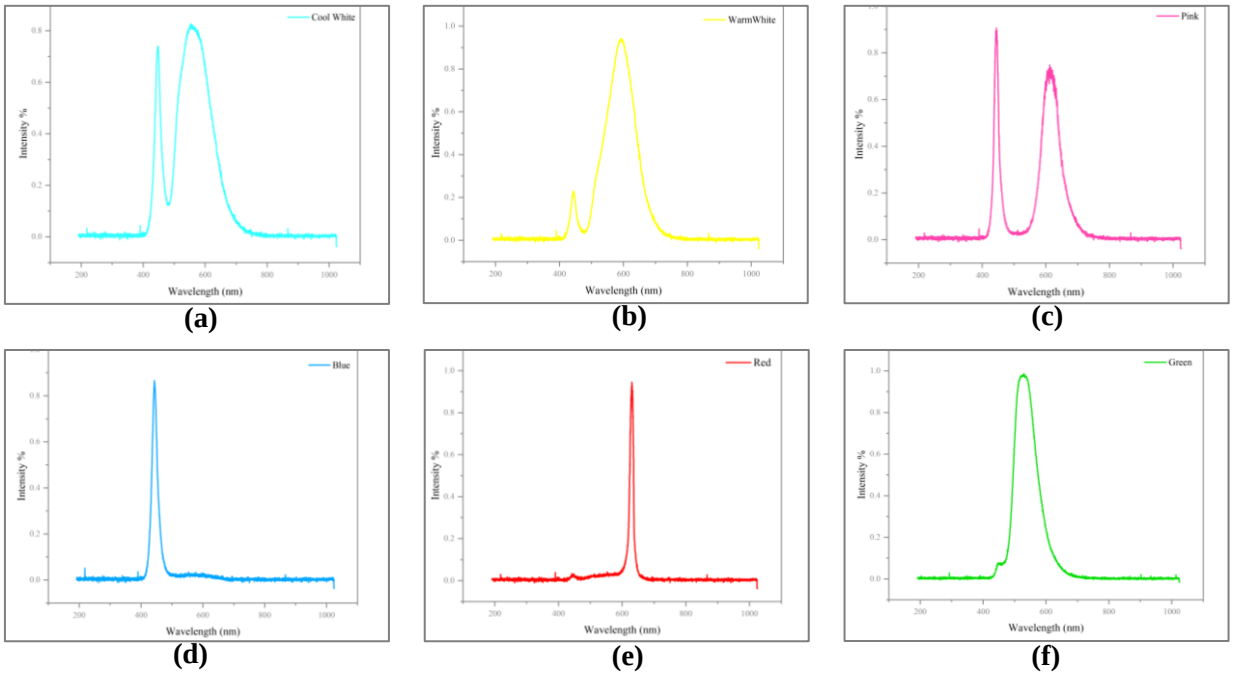

Figure 4B.1: Light spectrum of the LEDs measured using Compact CCD Spectrometer for **(a):** Cool-white LED **(b):** Warm white LED **(c):** Pink LED **(d):** Blue LED **(e):** Red LED and **(f):** Green LED.

Thus, cool-white, pink, blue, and red LEDs were used in the developed microalgae culture experimental setups, and optimization experimentations using response surface methodology were carried out, as described in the following sections.

4B.1.2 Light intensity of the four chosen LEDs at different power levels.

After development of the microalgae culture experimental setups and installation of the four selected LEDs to the setup the light intensities were measured at different power levels using

Apogee MQ-510 full spectrum quantum sensor. The light intensities against different power levels for the four LEDs are presented in Figure 4B.2.

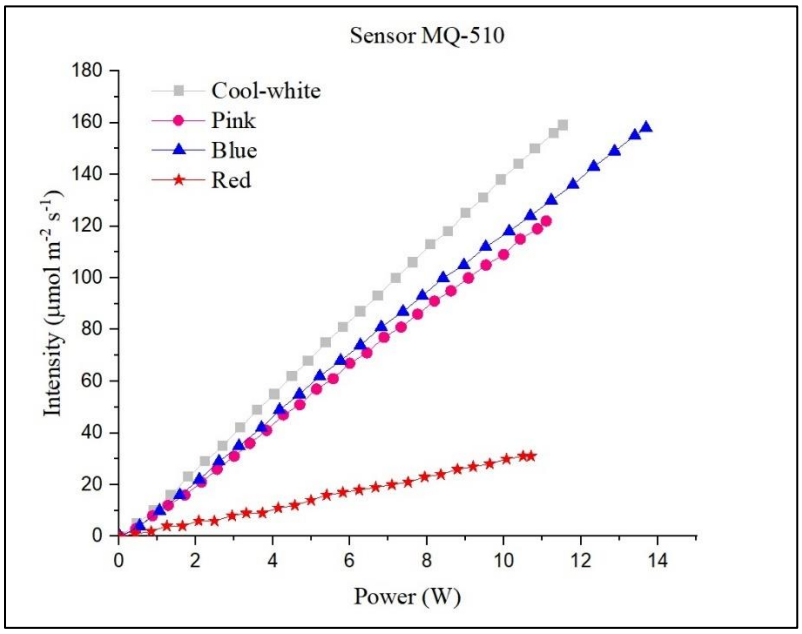

Figure 4B.2: Light intensity of the LEDs measured using Apogee MQ-510 full spectrum quantum sensor for Cool-white, Pink, Blue and Red LEDs installed in the microalgae culture experimental setup.

The MQ-510 is a quantum sensor that has a broader spectral response (400-700 nm) covering the entire visible radiation. This makes the MQ-510 more suitable for measuring the intensity of a wide range of LEDs. The quantum sensor measures the light intensity in terms of the number of photons hitting per unit surface per unit time and thus is expressed in µmol m^{-2} s^{-1} or µE m^{-2} s^{-1} [10]. As seen in the Figure 4B.2, the light intensity of cool-white LED illumination is the maximum followed by blue, pink and red LEDs at any given power level. The light intensity values can be correlated with the power level used for the optimization experimentations.

4B.2. Response surface methodology (RSM) based optimization of operational parameters for optimum biomass and lipid productivity

The growth and metabolism of microalgae are dependent on and affected by various parameters like light, carbon source, nitrogen content, temperature, pH, salinity, etc. Studies on the effect of single parameters like carbon sources [11], magnetic field stress [12], nitrogen content [13], on the growth and metabolism of *C. homosphaera* have been reported, but not much studies are found on the complex interactive effects of multiple parameters. The complexity arisen by the interactive

effect of different parameters such as light intensity, light wavelength, light duration, air flow rate and nitrogen content are investigated for optimum growth performance of the microalgae species. The study was done using the statistical experimental design method i.e. using design of experiment (DOE) methodology. A Face Centered Central Composite Design (FCCCD) based Response Surface Methodology (RSM) model is developed to optimize the LED illuminated microalgae culture conditions.

4B.2.1 Investigating the effect of input parameters on biomass productivity of *C homosphaera*.

The biomass production in response to light intensity, duration, airflow, and nitrogen concentrations were investigated. The ANOVA analysis in Table 4B.1 indicates a significant quadratic model ($p<0.001$). Meanwhile, Table 4B.2 compares model predictions with experimental outcomes. The F values (30.86, 53.28, 13.66, and 52.95) demonstrate model fit for cool-white, pink, blue, and red LEDs, respectively, with <0.001 probability. The analysis indicates that light duration and intensity significantly impact biomass output ($p <0.001$) in all four LED illuminations.

Under cool-white, pink, and red illumination, biomass productivity increased with light intensity, reaching maximum at 100% intensity. Using blue illumination, however, biomass productivity was maximum at 98% intensity, as shown in Figures 4B.5(a) and 4B.5(b), and biomass production slightly decreased with further increase in intensity. Increase in biomass productivity with increasing light intensity is supported by findings of Iasimone et al. [14], enlightening the increase in biomass productivity with increase in light intensity of a consortia of microalgae cultivated using wastewater. Similar findings were also reported by Nzayisenga et al. [15], where the biomass of *Desmodesmus* sp., *Chlorella vulgaris*, *Ettlia pseudoalveolaris* and *Scenedesmus obliquus* microalgae species increased with increase in light intensities. Microalgae growth keeps increasing with increase in light intensity till a certain level called the saturation light intensity, after that the microalga growth declines with increase in light intensity [16]. The saturation light intensity exhibits variability based on the specific microalgae species as well as the characteristics of the lighting [17]. The findings of this study suggest that cool-white, pink, and red LED illuminations have the potential to enhance biomass productivity further more. However, the existing limits of

the experimental settings prevented the intensity from being increased beyond 100%, thereby hindering the realization of this potential.

Along with the light intensity, light duration plays a significant role in the growth and metabolism of microalgae [18]. As evident from the current findings, apart from cool-white LED illumination, biomass productivity increased with illumination duration in all three (pink, blue, and red) LED illuminations, as shown in Figure 4B.4(a), 4B.4(c), 4B.4(e), 4B.5(a), 4B.5(c), 4B.5(e), 4B.6(a), 4B.6(c), and 4B.6(e) giving maximum productivity under continuous illumination. In cool-white LED illumination, biomass growth increased with illumination time to a point, peaking at 22.8 hours and declining after that (Figure 4B.3(a), 4B.3(c), and 4B.3(e)). Microalgae can be grown under continuous illumination [19], light dark illumination cycle [20] or under pulsating illumination [21]. The biochemical composition of microalgae is affected by the changes in the duration of light dark cycle. Depending on growth environment and microalgae strain, different photoperiods are proven to be beneficial [22]. In certain cases, continuous illumination produces better results [23], as evident in the present scenario with pink, blue and red LED illuminations. In certain cases, continuous illumination can cause photo inhibition, and thus a dark cycle even for a brief amount of period is necessary to restore the damage to the photosystem [24].

Maintaining nitrogen content at its optimum concentration is significant, as excessive nitrogen concentration causes growth inhibition [25] and inadequate or nitrogen depletion condition results in low biomass productivity [26]. Nitrogen enhances biomass growth and affects other metabolites. The present study reproduces similar findings. In cool-white and pink LED-illuminated culture, Figure 4B.3(b), 4B.3(c), 4B.3(f), 4B.4(b), 4B.4(c), and 4B.4(f), biomass growth gradually increases with increasing nitrogen concentration to reach a maximum at 1.61 g L^{-1} and 1.03 g L^{-1} for cool-white and pink LED illumination, respectively, and then decreases. The optimized maximum nitrogen content of 0.1 g L^{-1} in blue and red LED lighting maximized biomass productivity.

As evident from the ANOVA analysis in Table 4B.1, the influence of airflow on biomass growth is minimal in the present study. Airflow rates of 1.3, 1.44, 1.49, and 0.4 L min^{-1} for cool-white, pink, blue, and red LED illumination were found to result in maximum biomass productivity. Further insight about the effect of airflow on the biomass growth is presented in the following optimization section.

Table 4B.1: ANOVA analysis of biomass production using the four LED illuminations

Biomass Production													
Source	df	Cool white LED			Pink LED			Blue LED			Red LED		
		F-value	P=value Prof>F		F-value	P=value Prof>F		F-value	P=value Prof>F		F-value	P=value Prof>F	
Model	14	30.86	< 0.0001	Sig.	53.28	< 0.0001	Sig.	13.66	< 0.0001	Sig	52.95	< 0.0001	Sig
A- LI	1	95.17	< 0.0001		117.77	< 0.0001		18.69	0.0006		250.37	< 0.0001	
B- LD	1	135.60	< 0.0001		213.48	< 0.0001		117.78	< 0.0001		283.07	< 0.0001	
C-AF	1	1.96	0.1815		0.0261	0.8739		0.3702	0.5520		0.2036	0.6583	
D- Nitro	1	7.73	0.0140		12.44	0.0030		0.0017	0.9681		2.52	0.1333	
AB	1	6.11	0.0259		26.89	0.0001		2.77	0.1170		104.83	< 0.0001	
AC	1	2.27	0.1526		2.10	0.1675		0.3754	0.5492		0.1045	0.7510	
AD	1	4.64	0.0479		1.05	0.3215		0.0065	0.9369		1.75	0.2059	
BC	1	3.35	0.0871		0.1473	0.7066		0.3446	0.5659		1.04	0.3239	
BD	1	12.44	0.0030		9.36	0.0079		0.2530	0.6223		0.9403	0.3476	
CD	1	3.30	0.0895		0.2212	0.6449		0.0139	0.9077		0.0192	0.8917	
A^2	1	0.5543	0.4681		0.0704	0.7943		2.05	0.1728		7.25	0.0167	
B^2	1	18.10	0.0007		2.28	0.1522		1.64	0.2196		4.01	0.0636	
C^2	1	4.14	0.0600		3.52	0.0803		5.59	0.0320		2.95	0.1062	
D^2	1	7.26	0.0167		81.17	< 0.0001		0.1866	0.6719		0.0123	0.9133	
Lack of Fit	10	1.51	0.3397	N. Sig.	3.16	0.1083	N. Sig.	2.10	0.2135	N. Sig.	1.21	0.4405	N. Sig.
R^2		0.9664			0.9803			0.9273			0.9802		

LI= Light Intensity, LD= Light Duration, AF=Air flow, Nitro=Nitrogen, Sig. = significant, N. Sig. = not significant

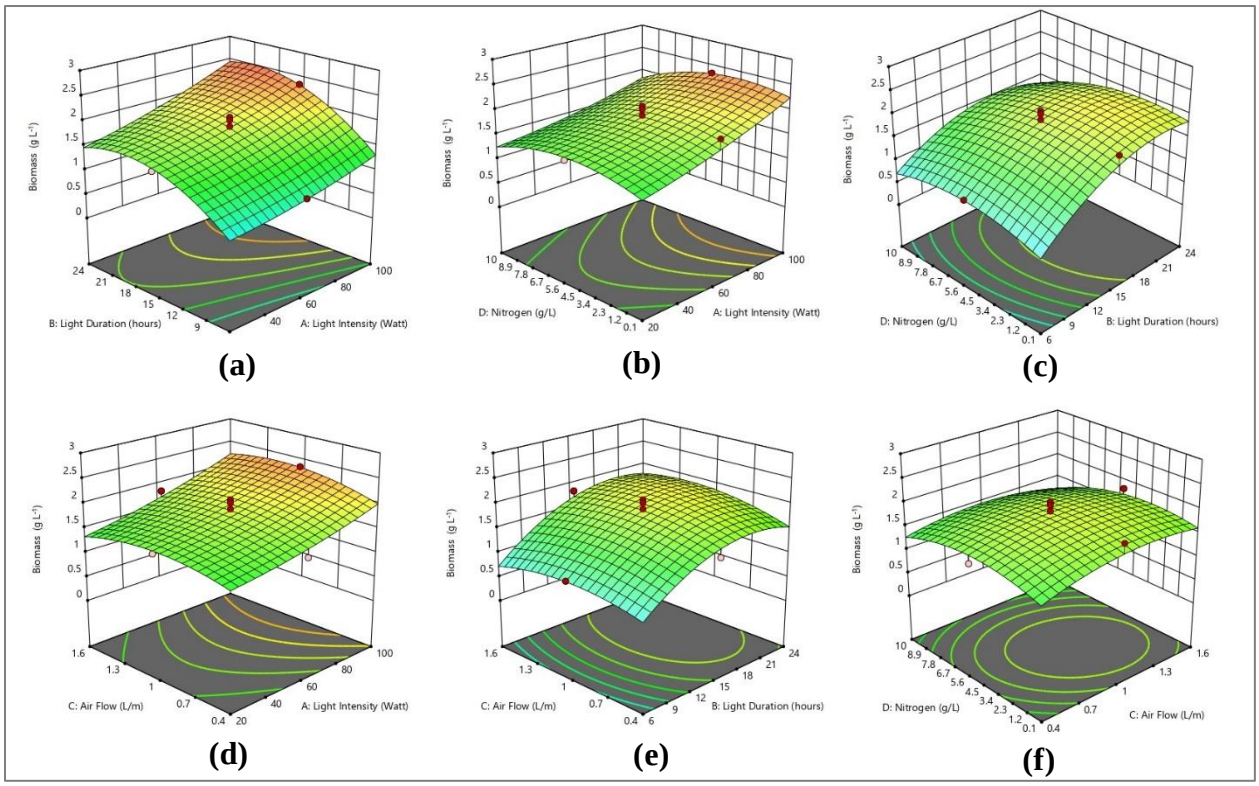

Fig 4B.3 (a-f): Effect of different parameters on the biomass growth cultured using Cool-white LED illumination.

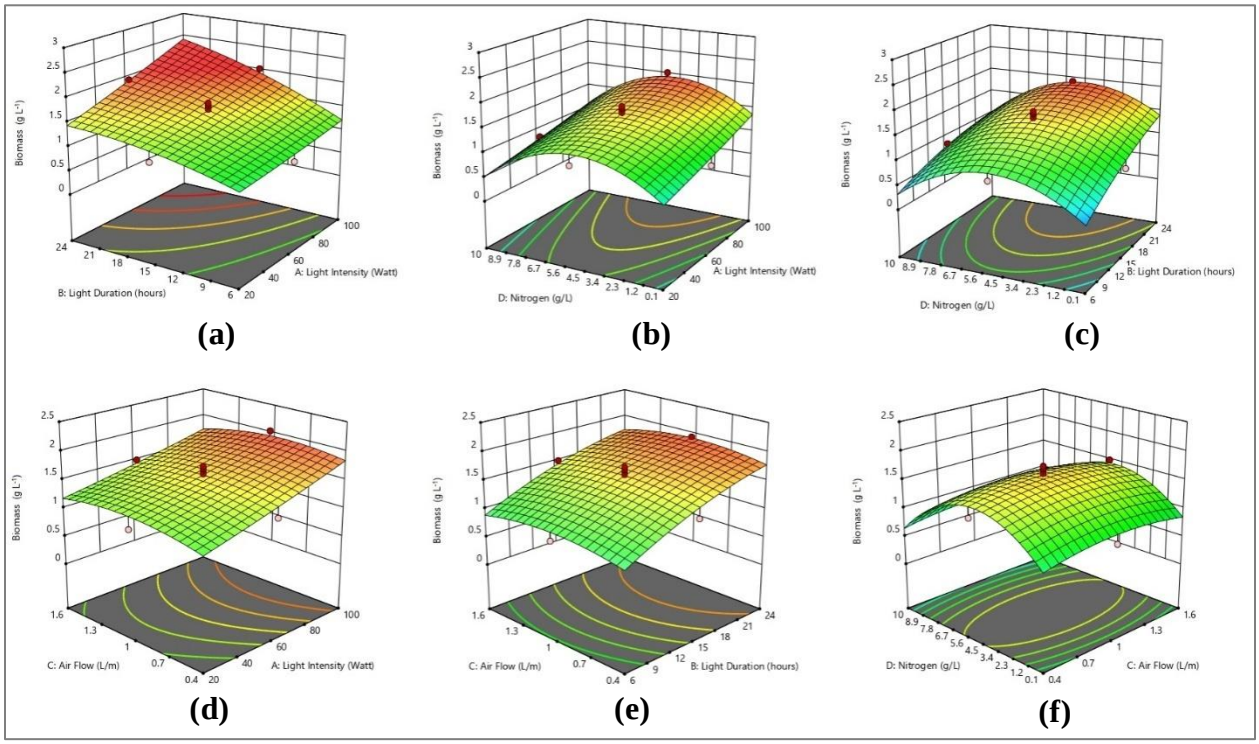

Fig 4B.4 (a-f): Effect of different parameters on the biomass growth cultured using Pink LED illumination.

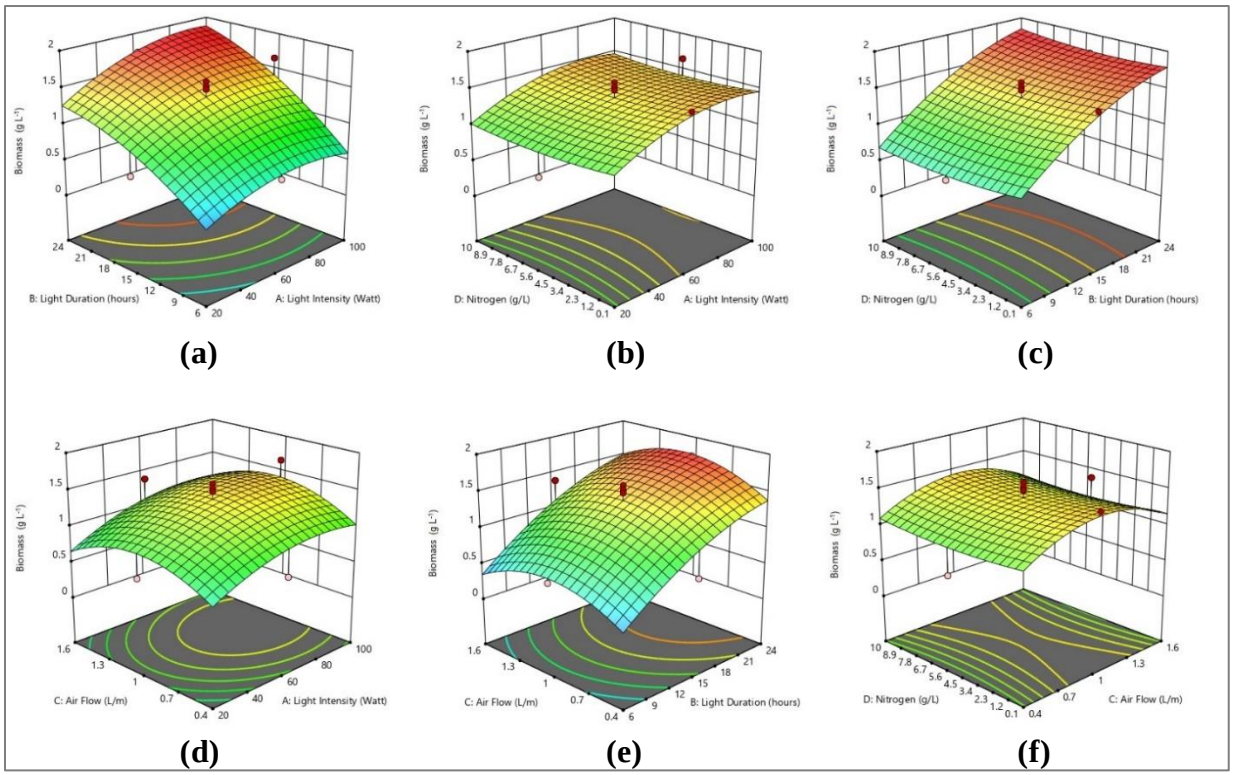

Figure 4B.5 (a-f): Effect of different parameters on the biomass growth cultured using Blue LED illumination.

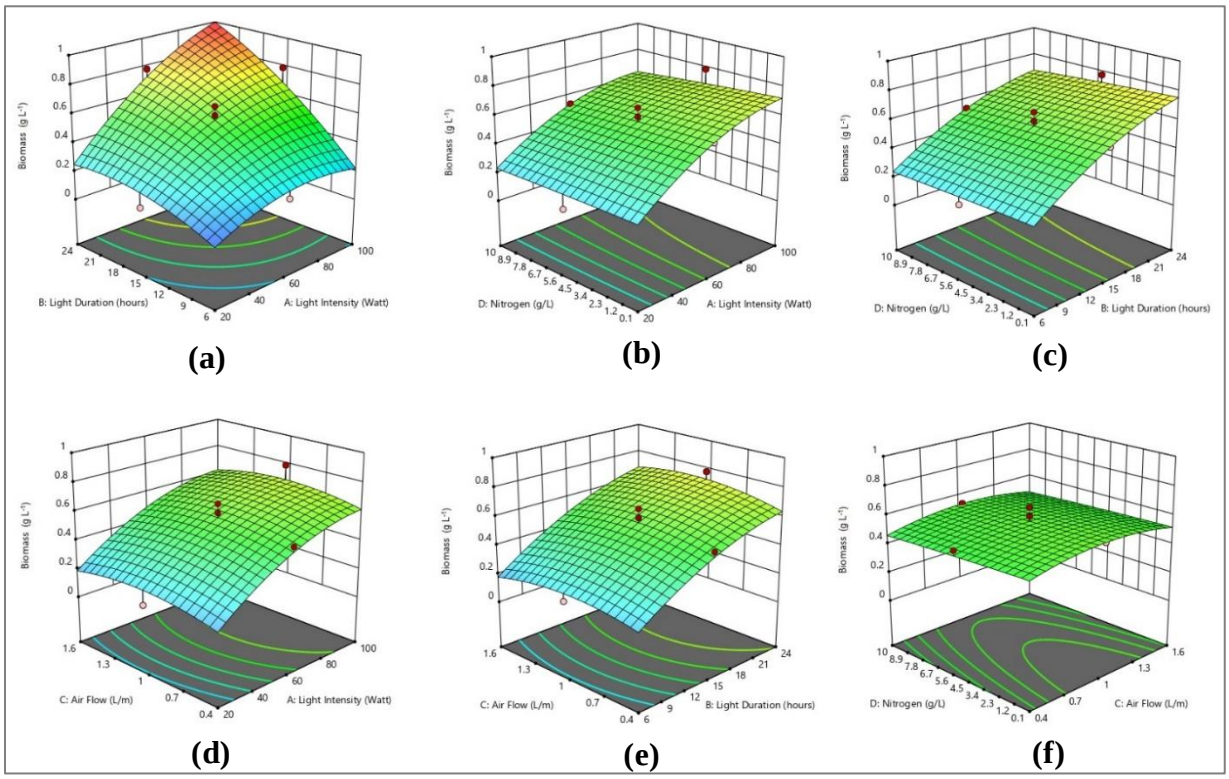

Figure 4B.6 (a-f): Effect of different parameters on the biomass growth cultured using Red LED illumination.

Table 4B.2: Predicted and experimental results of biomass productivity obtained in the RSM

Experimental parameters					Biomass Production (g L^{-1})							
					White		Pink		Blue		Red	
No	Int.	Dur.	Air	Nitro.	Exp.	Pred.	Exp.	Pred.	Exp.	Pred.	Exp.	Pred.
1	20	6	0.4	0.1	0.058	0.132	0.042	0.058	0.146	0.144	0.029	0.008
2	20	6	0.4	10	0.642	0.543	0.068	0.021	0.134	0.090	0.031	0.027
3	20	6	1.6	0.1	0.118	0.115	0.094	0.079	0.126	0.089	0.03	0.005
4	20	6	1.6	10	0.201	0.220	0.088	0.098	0.102	0.010	0.042	0.023
5	20	15	1	5.05	1.494	1.551	1.066	1.286	0.638	0.970	0.136	0.239
6	20	24	0.4	0.1	1.122	0.991	0.706	0.707	1.042	0.945	0.18	0.173
7	20	24	0.4	10	0.754	0.808	0.422	0.396	1.186	0.999	0.138	0.135
8	20	24	1.6	0.1	1.134	1.283	0.842	0.795	0.996	1.016	0.212	0.222
9	20	24	1.6	10	0.914	0.793	0.421	0.424	0.938	1.045	0.218	0.192
10	60	6	1	5.05	0.966	0.954	0.884	1.033	0.598	0.660	0.197	0.251
11	60	15	0.4	5.05	1.422	1.593	1.258	1.446	0.659	1.033	0.526	0.491
12	60	15	1	0.1	1.902	1.690	0.818	0.984	1.494	1.438	0.578	0.579
13	60	15	1	5.05	2.081	1.862	1.526	1.589	1.482	1.379	0.545	0.561
14	60	15	1	5.05	1.854	1.862	1.742	1.589	1.483	1.379	0.514	0.561
15	60	15	1	5.05	1.894	1.862	1.722	1.589	1.526	1.379	0.656	0.561
16	60	15	1	5.05	2.02	1.862	1.698	1.589	1.587	1.379	0.594	0.561
17	60	15	1	5.05	1.718	1.862	1.642	1.589	1.318	1.379	0.51	0.561
18	60	15	1	5.05	1.742	1.862	1.606	1.589	1.146	1.379	0.542	0.561
19	60	15	1	10	1.208	1.469	0.808	0.773	1.288	1.434	0.536	0.535
20	60	15	1.6	5.05	1.826	1.704	1.494	1.436	1.379	1.095	0.469	0.504
21	60	24	1	5.05	1.817	1.878	1.926	1.907	1.728	1.756	0.777	0.723
22	100	6	0.4	0.1	0.807	0.756	0.466	0.419	0.417	0.329	0.157	0.198
23	100	6	0.4	10	0.788	0.804	0.312	0.367	0.352	0.292	0.16	0.140
24	100	6	1.6	0.1	0.882	0.993	0.338	0.372	0.258	0.405	0.175	0.167
25	100	6	1.6	10	0.776	0.735	0.304	0.260	0.228	0.344	0.094	0.116
26	100	15	1	5.05	2.336	2.329	2.024	1.934	1.648	1.407	0.787	0.685
27	100	24	0.4	0.1	1.886	2.031	1.844	1.841	1.434	1.485	0.966	0.973
28	100	24	0.4	10	1.654	1.485	1.43	1.401	1.502	1.556	0.807	0.857
29	100	24	1.6	0.1	2.65	2.577	1.742	1.745	1.626	1.688	0.984	1.002
30	100	24	1.6	10	1.634	1.725	1.138	1.245	1.772	1.734	0.884	0.894

4B.2.2 Investigating the effect of input parameters on lipid productivity of *C homosphaera*

Effect on lipid productivity caused by different input parameters namely light intensity, light duration, airflow, and nitrogen concentrations were modeled. The quadratic model analyzed with ANOVA shown in Table 4B.3 shows the model to be significant ($p<0.001$). The F value (67.49, 47.42, 26.51 and 33.28) for the models (cool-white, pink, blue and red) with probability <0.001 ascertains the model fit. The lipid productivity in the culture increases with increase in the light duration. Highest lipid productivity of 384, 276, 239 and 232 mg L^{-1} were recorded with 24 hours of illumination in pink, blue, cool-white and red LED illumination respectively as seen in Table

4B.4, experiment number 29 for pink, cool-white, blue and experiment number 27 for red LED illumination.

Light intensity plays a similar role as that of light duration in case of lipid production. The optimized maximum lipid production was evaluated to be at 100% intensities in the case of cool-white, pink and red LEDs; and at 98% in case of blue LED illumination. The lipid production in blue LED culture dropped with further increase in intensity, as seen in Figure 4B.9(a).

Nitrogen is a crucial macronutrient having a significant influence in the growth and composition of microalgae, particularly its lipid content [27]. Low nitrogen content is favorable for lipid productivity [14]. The responses of the current investigation support the same, where lipid production in microalgae is significantly affected by nitrogen concentration. As seen in Figure 4B.6-4B.9, lipid productions were maximum in nitrogen limiting conditions. The highest lipid production in all the four LED illuminations, shown in Table 4B.4, were recorded at a nitrogen concentration of 0.1 g L^{-1}.

Initially the lipid production in all the LEDs increaser with increase in airflow, reached a maximum at a certain and started to fall with further increase in the air flow. The optimized airflows for maximum lipid production were estimated to be 1.3,1.43,1.48 and 0.4 L min^{-1} for cool-white, pink, blue and red LED illuminations, respectively.

The effect of nitrogen and airflow in the lipid productivities are further discussed in the optimization section that follows.

Table 4B.3: ANOVA analysis of lipid production using the four LED illuminations

Lipid Production													
Source	df	Cool white			Pink			Blue			Red		
		F-value	P=value Prof>F		F-value	P=value Prof>F		F-value	P=value Prof>F		F-value	P=value Prof>F	
Model	14	67.49	< 0.0001	Sig.	47.42	< 0.0001	Sig.	26.51	< 0.0001	Sig.	33.28	< 0.0001	Sig.
A-LI	1	280.76	< 0.0001		220.53	< 0.0001		57.64	< 0.0001		93.58	< 0.0001	
B-LD	1	367.99	< 0.0001		279.95	< 0.0001		226.72	< 0.0001		284.32	< 0.0001	
C-AF	1	10.99	0.0047		21.85	0.0003		6.76	0.0201		6.37	0.0234	
D-Nitro	1	20.15	0.0004		29.95	< 0.0001		4.27	0.0565		3.51	0.0806	
AB	1	12.36	0.0031		44.44	< 0.0001		14.92	0.0015		11.06	0.0046	
AC	1	1.42	0.2524		2.24	0.1553		4.42	0.0528		3.33	0.0880	
AD	1	22.41	0.0003		25.04	0.0002		5.21	0.0375		7.16	0.0172	
BC	1	8.13	0.0121		10.96	0.0048		6.97	0.0186		2.25	0.1542	
BD	1	12.36	0.0031		2.62	0.1266		3.04	0.1015		10.01	0.0064	
CD	1	3.65	0.0754		1.22	0.2872		6.66	0.0209		16.12	0.0011	
A^2	1	13.04	0.0026		0.3602	0.5573		10.03	0.0064		13.73	0.0021	
B^2	1	0.5703	0.4618		0.0129	0.9111		1.44	0.2484		3.53	0.0799	
C^2	1	36.21	< 0.0001		3.85	0.0685		1.22	0.2873		0.5372	0.4749	
D^2	1	0.0507	0.8249		0.3602	0.5573		0.1859	0.6725		7.96	0.0129	
Lack of Fit	10	3.97	0.0706	N. Sig.	3.66	0.0825	N. Sig.	4.14	0.0651	N. Sig.	3.12	0.1108	N. Sig.
R^2			0.9844			0.9779			0.9612			0.9688	

LI= Light Intensity, LD= Light Duration, AF=Air flow, Nitro= Nitrogen, Sig. = significant, N. Sig. = not significant

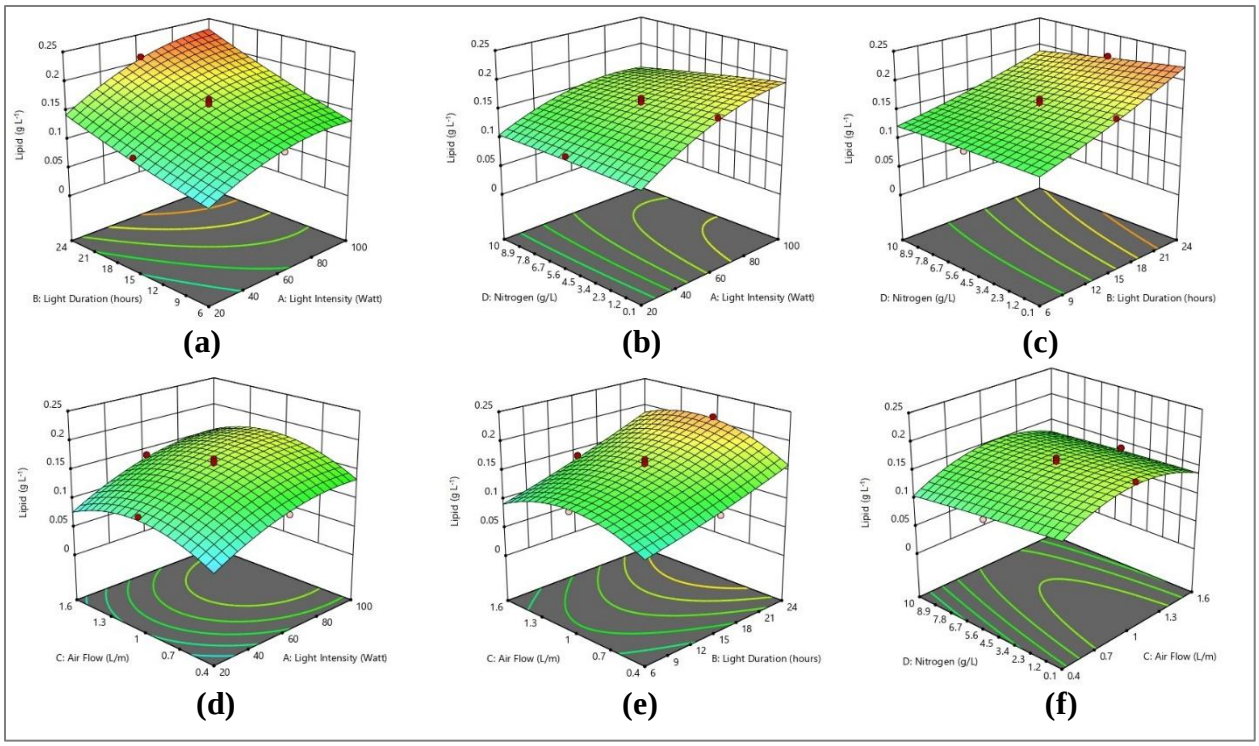

Figure 4B.7 (a-f): Effect of different parameters on the lipid production for microalgae cultured using Cool-white LED illumination.

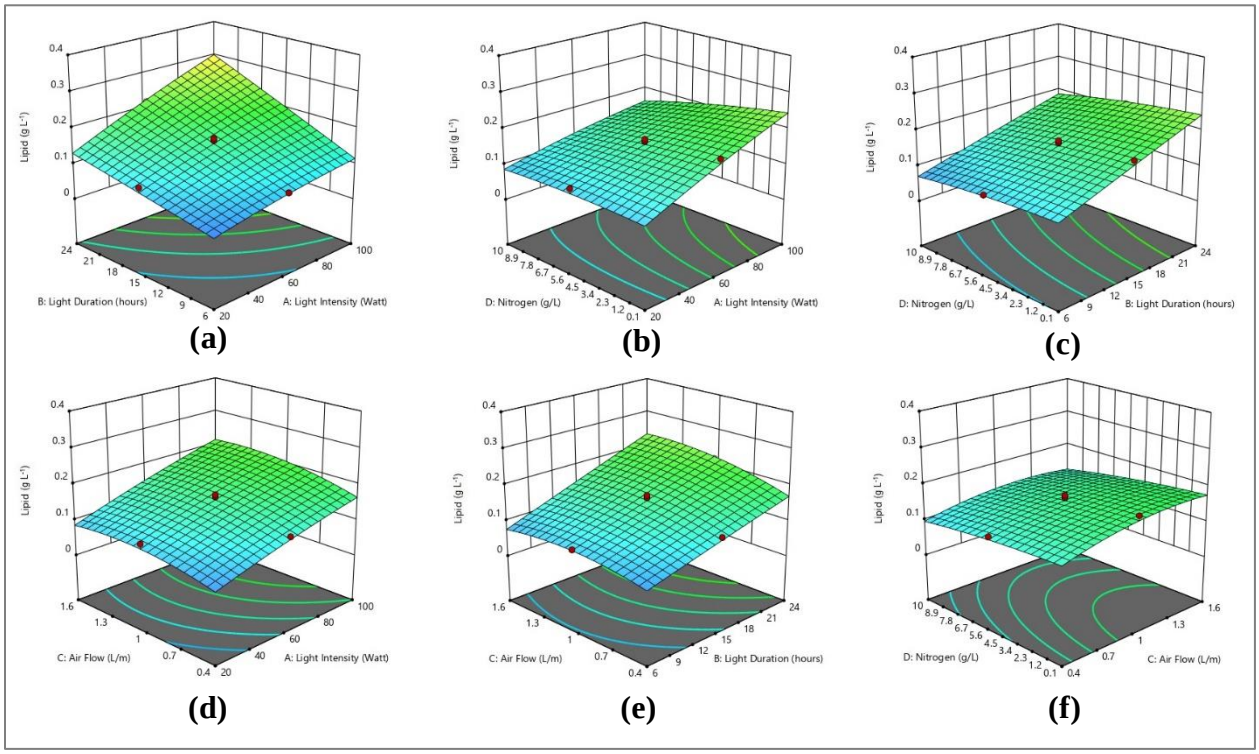

Figure 4B.8 (a-f): Effect of different parameters on the lipid production for microalgae cultured using Pink LED illumination.

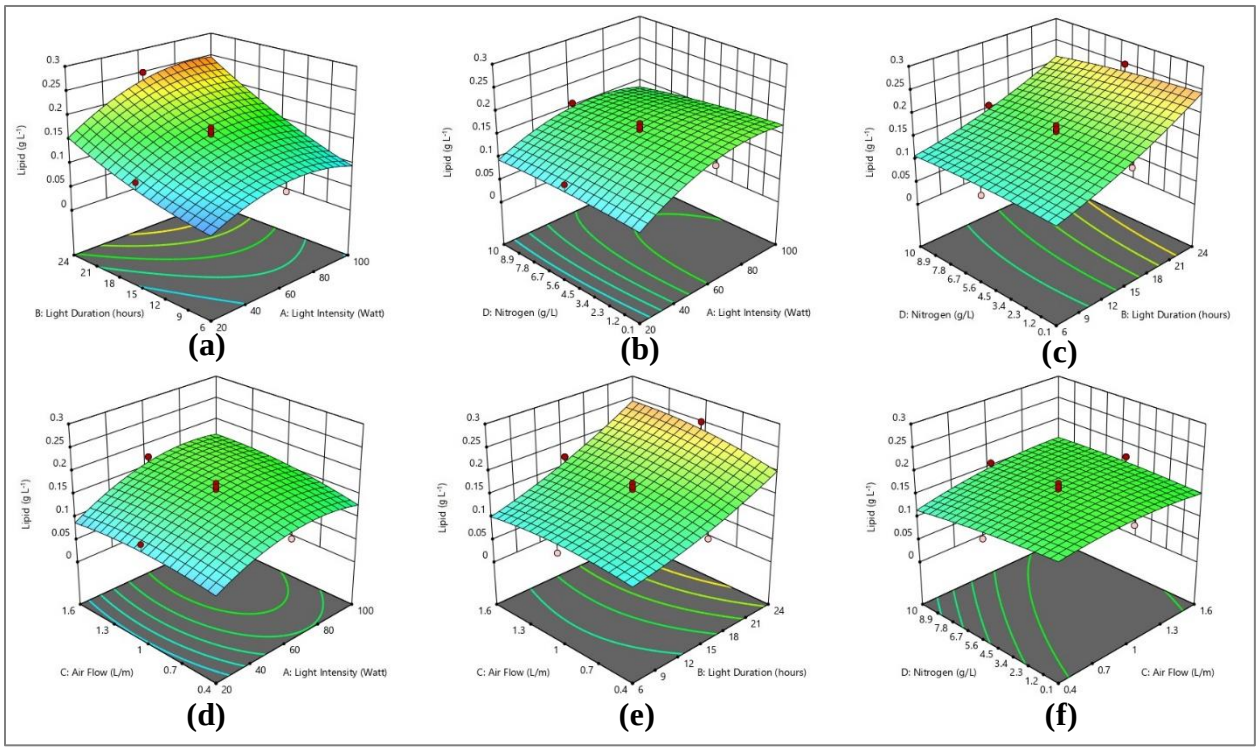

Figure 4B.9 (a-f): Effect of different parameters on the lipid production for microalgae cultured using Blue LED illumination.

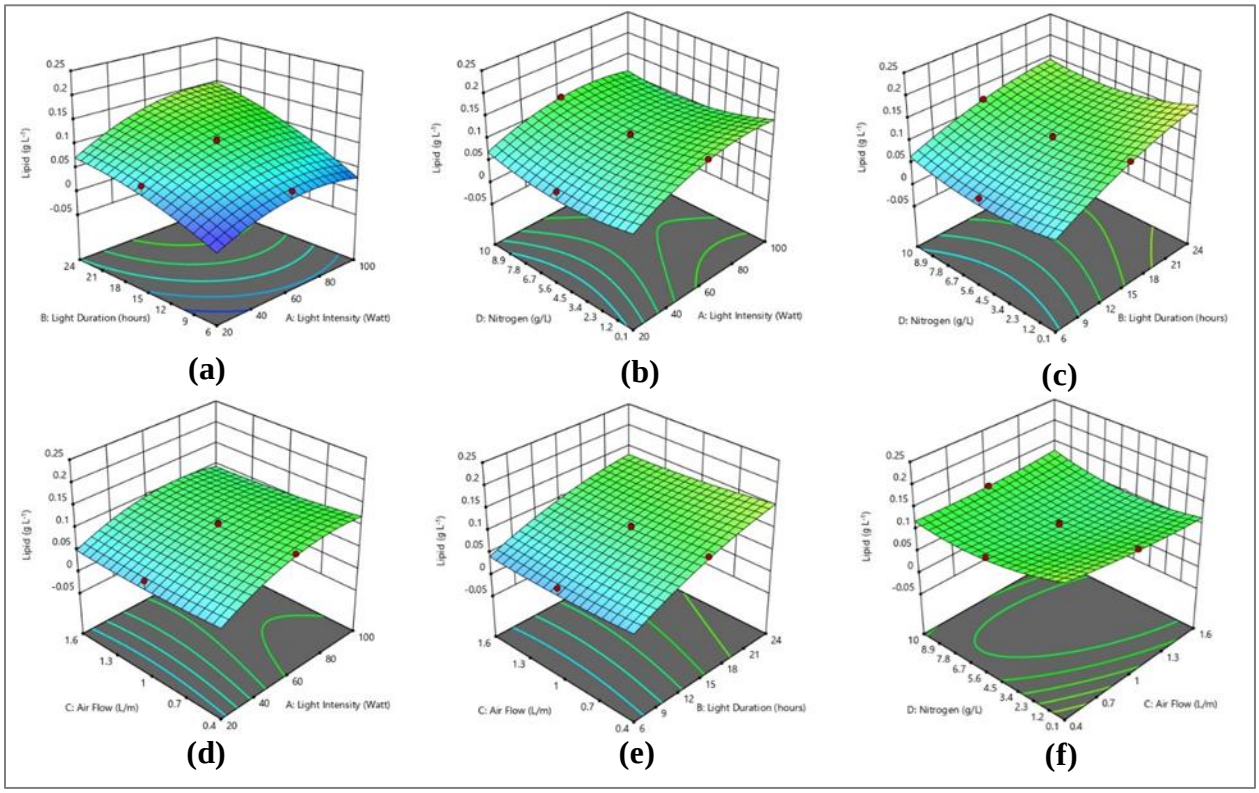

Figure 4B.10 (a-f): Effect of different parameters on the lipid production for microalgae cultured using Red LED illumination.

Table 4B.4: Predicted and experimental results of lipid productivity obtained in the RSM experiments.

Experimental parameters					Lipid Production (mg L^{-1})							
					White		Pink		Blue		Red	
No	Int.	Dur.	Air	Nitro.	Exp.	Pred.	Exp.	Pred.	Exp.	Pred.	Exp.	Pred.
1	20	6	0.4	0.1	26.0	40.0	18.0	19.0	52.0	64.0	9.0	18.0
2	20	6	0.4	10	51.0	49.0	22.0	41.0	62.0	59.0	18.0	18.0
3	20	6	1.6	0.1	35.0	27.0	38.0	25.0	45.0	23.0	7.0	1.0
4	20	6	1.6	10	56.0	53.0	26.0	28.0	50.0	62.0	34.0	49.0
5	20	15	1	5.05	112.0	106.0	107.0	94.0	114.0	99.0	66.0	47.0
6	20	24	0.4	0.1	116.0	108.0	72.0	81.0	144.0	142.0	124.0	124.0
7	20	24	0.4	10	90.0	86.0	92.0	76.0	116.0	109.0	84.0	85.0
8	20	24	1.6	0.1	114.0	121.0	124.0	142.0	132.0	146.0	78.0	86.0
9	20	24	1.6	10	108.0	116.0	122.0	118.0	146.0	156.0	106.0	97.0
10	60	6	1	5.05	122.0	124.0	94.0	91.0	96.0	114.0	56.0	39.0
11	60	15	0.4	5.05	116.0	120.0	127.0	120.0	126.0	139.0	122.0	115.0
12	60	15	1	0.1	175.0	169.0	186.0	173.0	154.0	164.0	134.0	129.0
13	60	15	1	5.05	170.0	161.0	166.0	158.0	168.0	160.0	92.0	102.0
14	60	15	1	5.05	166.0	161.0	154.0	158.0	148.0	160.0	108.0	102.0
15	60	15	1	5.05	155.0	161.0	150.0	158.0	162.0	160.0	98.0	102.0
16	60	15	1	5.05	160.0	161.0	172.0	158.0	176.0	160.0	94.0	102.0
17	60	15	1	5.05	160.0	161.0	148.0	158.0	166.0	160.0	108.0	102.0
18	60	15	1	5.05	162.0	161.0	166.0	158.0	158.0	160.0	110.0	102.0
19	60	15	1	10	146.0	150.0	113.0	131.0	158.0	148.0	120.0	118.0
20	60	15	1.6	5.05	140.0	134.0	144.0	156.0	172.0	159.0	100.0	100.0
21	60	24	1	5.05	210.0	206.0	215.0	223.0	250.0	232.0	126.0	136.0
22	100	6	0.4	0.1	125.0	108.0	104.0	109.0	106.0	89.0	84.0	79.0
23	100	6	0.4	10	80.0	74.0	66.0	48.0	62.0	47.0	46.0	46.0
24	100	6	1.6	0.1	100.0	106.0	124.0	140.0	78.0	83.0	30.0	37.0
25	100	6	1.6	10	91.0	90.0	68.0	61.0	90.0	85.0	68.0	54.0
26	100	15	1	5.05	171.0	174.0	192.0	210.0	141.0	155.0	88.0	100.0
27	100	24	0.4	0.1	204.0	208.0	284.0	282.0	246.0	233.0	232.0	225.0
28	100	24	0.4	10	144.0	143.0	179.0	194.0	146.0	161.0	160.0	153.0
29	100	24	1.6	0.1	239.0	232.0	384.0	367.0	276.0	271.0	180.0	165.0
30	100	24	1.6	10	196.0	184.0	262.0	261.0	256.0	243.0	144.0	142.0

4B.2.3 Modeling and validation

The experimental design parameters were analyzed by Design Expert software and fitted to quadratic polynomial equations. High regression coefficient (R^2) of 0.97, 0.98, 0.93 and 0.98 for biomass productivity using cool-white (Y_1), pink (Y_2), blue (Y_3) and red (Y_4) were achieved, and in case of lipid productivity R^2 of 0.98, 0.98, 0.96 and 0.97 were achieved using cool-white (Y_5), pink (Y_6), blue (Y_7) and red (Y_8) LED illumination, respectively. The quadratic model equations (Eq. 4B.1-4B.8) obtained are as follows:

Y_1= -1.31- 0.01A + 0.20B + 1.03C + 0.20D + 0.01AB + 0.01AC -0.01AD + 0.01BC -0.01BD -0.03CD + 0.01A^2-0.01B^2-0.59C^2-0.01D^2 Eq. 4B.1

Y_2 = -0.92 + 0.01A + 0.08B + 0.98C + 0.32D + 0.01AB -0.01AC -0.01 AD -0.01BC -0.01BD -0.01CD + 1.31A^2-0.01B^2-0.41C^2- 0.03D^2 Eq. 4B.2

Y_3 = -1.19 + 0.01A + 0.10B + 1.64C -0.03D + 0.01AB + 0.01AC + 2.18AD + 0.01BC +0.01BD -0.01 CD -0.01A^2-0.01B^2-0.87C^2 + 0.01D^2 Eq. 4B.3

Y_4 = -0.40 + 0.01A + 0.03B + 0.33C + 0.01D + 0.01AB -0.01AC -9.94AD + 0.01BC -0.01BD + 0.01CD -6.22A^2-0.01B^2- 0.18C^2-0.0D^2 Eq. 4B.4

Y_5 = 0.16 + 0.04A + 0.04B + 0.01C -0.01D + 0.01AB + 0.01AC -0.01AD + 0.01BC -0.01BD + 0.01CD -0.02A^2 + 0.01B^2-0.03C^2- 0.01D^2 Eq. 4B.5

Y_6 = -0.05 + 0.01A + 0.01B + 0.09C + 0.01C + 7.65D + 0.01AB -0.01AC + 0.01BC -0.01BD -0.01CD -3.85A^2-1.44B^2 -0.06C^2-0.01D^2 Eq. 4B.6

Y_7 = 0.02 + 0.01A - 0.01B + 0.01C + 0.01D + 4.49AB + 0.01AC -4.83AD + 0.01BC -0.01BD + 0.01CD -2.06A^2 + 0.01B^2-0.03C^2-0.01D^2 Eq. 4B.7

Y_8 = -0.08 + 0.01A + 0.01B -0.04C -0.01D + 2.85AB -0.01AC - 4.17AD -0.01BC -0.01BD + 0.01CD -1.77A^2-0.01B^2 + 0.01C^2 + 0.01D^2 Eq. 4B.8

The lack of fit for all the models was insignificant, as shown in Tables 4B.1 and 4B.3. ANOVA analysis for all the eight models developed are significant (<0.0001). These results indicate the developed models strongly fit and correlate input parameters and the corresponding responses, and could efficiently explain the experimental data.

4B.2.4 Optimization of the input parameters

The optimum conditions to obtain the maximum response of biomass and lipid production, within the range of the input variables were predicted based on the developed model using the Design Expert software. The predicted values to obtain the maximum response with highest desirability were considered and the conditions were validated experimentally. The optimum conditions to obtain highest biomass and lipid content for the four LED illuminations are listed in Table 4B.5. The optimum conditions predicted were validated experimentally by conducting experiments in triplicate and comparing the mean results of the experiments with the predicted responses. The

biomass and lipid production obtained under the optimum conditions were also compared with results of microalgae culture obtained under normal conditions without any optimization that were published earlier [28]. The responses of biomass and lipid production obtained theoretically (predicted), experimentally and obtained under normal conditions are shown in Table 4B.5. The error in the predicted and experimental values for the biomass are 3.21%, 0.86%, 3.55% and 2.48% and for lipid are 4.23%, 2.01%, 1.66% and 5.63% for cool-white, pink blue and red LED illumination, respectively, indicating the developed model is accurate in predicting the growth of microalgae *C. homosphaera*.

Biomass production in the optimized condition and normal condition increased 1.30, 1.07, 1.01 and 1.13 folds in case of cool-white, pink, blue and red LED illumination, respectively. In case of lipid production under optimized and normal conditions there was an increase of 1.50, 1.81, 1.57 and 1.64 folds under cool-white, pink, blue and red LED illumination, respectively. Thus, the developed models were able to optimize the culture conditions and increase the biomass and lipid production successfully.

This is evident with the blue LED illumination, where the biomass productivity peaked at 98% illumination resulting in biomass productivity of 342.66 ± 3.53 mg L^{-1} day^{-1}, and further increase in light intensity reduced the biomass productivity. In case of cool-white, pink and red LED illumination the peak biomass productivity of 512.0 ± 12.23, 401.33 ± 10.48 and 189.6 ± 1.36 mg L^{-1} day^{-1} were achieved with 100% intensity, making cool-white the most preferred LED illumination in terms of biomass productivity.

Furthermore, from Table 4B.5, it is observed that white LED illumination results in maximum biomass productivity with a light: dark cycle of 22.8:1.2 hours. Introduction of dark period in an artificially illuminated microalgae culture has a major advantage, i.e., it saves energy. White LED in this case not only dominates in terms of biomass productivity, moreover it consumes lesser energy to do so as compared to the other three LED illuminations. Thus, in terms of energy consumption as well, calculated by multiplying power consumption(W) for maximum biomass productivity with illumination duration per day (h), cool-white (228.6 Wh day^{-1}) LED is the best option over pink (240.0 Wh day^{-1}), blue (235.05 Wh day^{-1}) and red (240.0 Wh day^{-1}) for biomass production of *C. homosphaera*.

Considering lipid productivity, the most preferred LED illumination to achieve highest lipid productivity in *C. homosphaera* is pink LED illumination resulting in lipid productivity of 69.8 ± 1.1 mg L^{-1} day^{-1} followed by blue (54.2 ± 1.01 mg L^{-1} day^{-1}), cool-white (45.86 ± 1.73 mg L^{-1} day^{-1}) and red (43.3 ± 1.59 mg L^{-1} day^{-1}) LED illumination.

As derived from Table 4B.5, nitrogen limiting condition (0.1 g L^{-1}) combined with red LED illumination produces the maximum lipid content (22.83%) amongst cool-white (8.95%), pink (17.39%) and blue (15.81%) LED illumination. Nevertheless, the biomass productivity observed under red LED illumination is the lowest among the four LEDs, leading to a minimum daily lipid productivity of 43.3 ± 1.59 mg L^{-1} day^{-1} under red LED illumination, which is also the lowest among the four LEDs. The pink LED illumination, when combined with a nitrogen concentration of 1.02 g L^{-1}, demonstrates the highest daily lipid productivity of 69.8 ± 1.1 mg L^{-1} day^{-1}. Therefore, it can be concluded that the pink LED illumination with the optimal nitrogen content outperforms the other three LED options in terms of lipid productivity. Similar findings were reported by Markou Giorgos [29], obtaining highest productivity of *Arthrospira platensis* microalgae culture using pink LED illumination. The advantage of pink LED can be attributed by the fact that, pink color is the combination of two primary color spectrums red and blue [28], where the blue component is known to supports biomass growth [9], while the red component encourages lipid productivity [30]. This is supported by the findings of Sirisuk et al. [31], where maximum productivity of *Isochrysis galbana* and *Phaeodactylum tricornutum* were obtained using a 50:50 mixture of blue and red LED illumination.

Carbon being over 50% of the microalgae biomass [32], is the most essential element needed during microalgae cultivation. In photo-autotrophic mode of cultivation, CO_2 is the most preferred carbon source [32]. Typically, while growing microalgae, CO_2 is supplied by bubbling ambient air through the culture media with or without adding supplementary CO_2 in the airflow. While providing ambient air without supplementing with CO_2, the flow rate of the air plays a vital role in the microalgae growth, as a low air flow rate will limit the available CO_2 required by the microalgae. At the same time, excessive airflow might result in building up hazardous sheer stress, damaging the microalgae culture [32]. The desired level of CO_2 in the system depends on carbon fixation rates, which are affected by factors influencing microalgae growth, like properties of growth light, nitrogen concentration, temperature, pH, etc. [33]. The experimental findings demonstrate a clear correlation between LED illuminations (cool-white, pink, blue, and red) and

their respective air flow rates. Notably, cool-white (512.0 ± 12.23 mg L^{-1} day^{-1}), pink (401.33 ± 10.48 mg L^{-1} day^{-1}), and blue (342.66 ± 3.53 mg L^{-1} day^{-1}) LED illuminations yield significantly higher biomass compared to red (189.6 ± 1.36 mg L^{-1} day^{-1}) LED illumination, resulting in a markedly lower air flow rate (0.40 L min^{-1}) for the latter. To conduct a comprehensive analysis of the CO_2 requirement and ascertain the airflow rate afterward, employing more advanced experimental methodologies will be necessary. These refined approaches can be implemented in future investigations.

4B.3 Implementing the optimized values in the STAMP system

The developed STAMP system was operated using optimized process parameters for two LED illuminations, cool-white and pink LEDs. Biomass productivity of 0.45 ± 0.01 $gL^{-1}day^{-1}$ and 0.36 ± 0.01 $gL^{-1}day^{-1}$ were obtained using cool-blue and pink LEDs, respectively. Biomass productivity improved 2.04 folds using the optimized parameter compared to initial productivity of 0.22 $gL^{-1}day^{-1}$ using normal operating conditions. Biomass productivity is in the range of commercially used tubular photobioreactor systems, reported to achieve 0.5 $gL^{-1}day^{-1}$ by Tan et al. [34]. The biomass productivity of the STAMP can increase many folds with further design optimizations and the addition of a carbon source.

The lipid productivity of 0.043 ± 0.001 $gL^{-1}day^{-1}$ and 0.064 ± 0.001 $gL^{-1}day^{-1}$ were obtained using cool-white and pink LED illumination, respectively. The lipid productivity obtained using pink LED illumination was higher than that of 0.053 $gL^{-1}day^{-1}$ obtained by Bredda et al. [35] growing *Dunaliella salina* using 65% blue and 35% green light illumination. The STAMP has further scope for improvement in biomass and lipid productivity.

Table 4B.5: Biomass and lipid content obtained using optimized conditions and normal conditions.

LED	Optimized conditions				Biomass ($mg\ L^{-1}\ day^{-1}$)			Lipid ($mg\ L^{-1}\ day^{-1}$)		
	Intensity (%)	Duration (hours)	Air flow ($L\ min^{-1}$)	Nitrogen ($g\ L^{-1}$)	Pred.	Exp.	N. C.	Pred.	Exp.	N. C.
White	100.00	22.86	1.31	1.60	528.442	512.0 ± 12.23	383.33± 22.12	47.802	45.86 ± 1.73	30.53 ± 3.20
Pink	100.00	24	1.44	1.02	404.802	401.33± 10.48	384.33 ± 8.26	71.23	69.8 ± 1.1	38.4 ± 0.69
Blue	97.94	24	1.49	0.1	354.832	342.66 ± 3.53	339.33± 12.36	55.14	54.2 ± 1.01	34.4 ±1.22
Red	100.00	24	0.40	0.1	194.342	189.6 ± 1.36	166.33 ± 6.12	45.748	43.3 ± 1.59	26.4 ± 1.9

Pred. = Predicted; Exp. = Experimental; N.C.= Normal Condition

4B.4. Summary

A comparative analysis of LED illuminated microalgae culture using RSM and FCCCD approach was conducted on different LEDs. Among the four LEDs, cool-white LED produced the highest biomass of 512.0 ± 12.23 mg L^{-1} day^{-1} and consumed the least energy of 228.6 Wh day^{-1}. At the same time, during the experimental analysis, Pink LED performed the best in terms of lipid productivity (69.8 ± 1.1 mg L^{-1} day^{-1}) at a nitrogen concentration of 1.02 g L^{-1} and with energy consumption of 240.0 Wh day^{-1}. Using the optimized culture parameters, the microalgae biomass productivity improved 2.04 folds in the STAMP system.

References

[1] Kim, C.W., et al., *Effect of monochromatic illumination on lipid accumulation of Nannochloropsis gaditana under continuous cultivation.* Bioresource technology, 2014. **159**: p. 30-35. DOI: https://doi.org/10.1016/j.biortech.2014.02.024.

[2] Kim, T.-H., et al., *The effects of wavelength and wavelength mixing ratios on microalgae growth and nitrogen, phosphorus removal using Scenedesmus sp. for wastewater treatment.* Bioresource technology, 2013. **130**: p. 75-80. DOI: https://doi.org/10.1016/j.biortech.2012.11.134.

[3] Baba, M., et al., *Wavelength specificity of growth, photosynthesis, and hydrocarbon production in the oil-producing green alga Botryococcus braunii*. Bioresource technology, 2012. **109**: p. 266-270. DOI: https://doi.org/10.1016/j.biortech.2011.05.059.

[4] Wang, S.K., et al., *Microalgae cultivation in photobioreactors: An overview of light characteristics.* Engineering in Life Sciences, 2014. **14**(6): p. 550-559. DOI: https://doi.org/10.1002/elsc.201300170.

[5] Schulze, P.S., et al., *Light emitting diodes (LEDs) applied to microalgal production.* Trends in biotechnology, 2014. **32**(8): p. 422-430. DOI: https://doi.org/10.1016/j.tibtech.2014.06.001.

[6] de Mooij, T., et al., *Impact of light color on photobioreactor productivity.* Algal research, 2016. **15**: p. 32-42. DOI: http://dx.doi.org/10.1016/j.algal.2016.01.015.

[7] Wilhelm, C., P. Krámer, and A. Wild, *Effect of different light qualities on the ultrastructure, thylakoid membrane composition and assimilation metabolism of Chlorella fusca.* Physiologia Plantarum, 1985. **64**(3): p. 359-364. DOI: https://doi.org/10.1111/j.1399-3054.1985.tb03353.x.

[8] Ritchie, R.J. and S. Sma-Air, *Microalgae grown under different light sources.* Journal of Applied Phycology, 2023. **35**(2): p. 551-566. DOI: https://doi.org/10.1007/s10811-023-02917-0.

[9] Jung, J.-H., et al., *Effects of green LED light and three stresses on biomass and lipid accumulation with two-phase culture of microalgae.* Process biochemistry, 2019. **77**: p. 93-99. DOI: https://doi.org/10.1016/j.procbio.2018.11.014.

[10] Gendron, F., C. Messier, and P.G. Comeau, *Comparison of various methods for estimating the mean growing season percent photosynthetic photon flux density in forests.* Agricultural and Forest Meteorology, 1998. **92**(1): p. 55-70. DOI: https://doi.org/10.1016/S0168-1923(98)00082-3.

[11] de Freitas, B.C.B., et al., *Cultivation of different microalgae with pentose as carbon source and the effects on the carbohydrate content.* Environmental technology, 2019. **40**(8): p. 1062-1070. DOI: https://doi.org/10.1080/09593330.2017.1417491.

[12] Costa, S.S., et al., *Increased lipid synthesis in the culture of Chlorella homosphaera with magnetic fields application.* Bioresource Technology, 2020. **315**: p. 123880. DOI: https://doi.org/10.1016/j.biortech.2020.123880.

[13] Margarites, A.C., et al., *Spirulina platensis is more efficient than Chlorella homosphaera in carbohydrate productivity.* Environmental technology, 2017. **38**(17): p. 2209-2216. DOI: https://doi.org/10.1080/09593330.2016.1254685.

[14] Iasimone, F., et al., *Effect of light intensity and nutrients supply on microalgae cultivated in urban wastewater: Biomass production, lipids accumulation and settleability characteristics.* Journal of environmental management, 2018. **223**: p. 1078-1085. DOI: https://doi.org/10.1016/j.jenvman.2018.07.024.

[15] Nzayisenga, J.C., et al., *Effects of light intensity on growth and lipid production in microalgae grown in wastewater.* Biotechnology for Biofuels, 2020. **13**: p. 1-8. DOI: https://doi.org/10.1186/s13068-019-1646-x.

[16] Wahidin, S., A. Idris, and S.R.M. Shaleh, *The influence of light intensity and photoperiod on the growth and lipid content of microalgae Nannochloropsis sp.* Bioresource technology, 2013. **129**: p. 7-11. DOI: https://doi.org/10.1016/j.biortech.2012.11.032.

[17] Bialevich, V., V. Zachleder, and K. Bišová, *The effect of variable light source and light intensity on the growth of three algal species.* Cells, 2022. **11**(8): p. 1293. DOI: https://doi.org/10.3390/cells11081293.

[18] Maltsev, Y., et al., *Influence of light conditions on microalgae growth and content of lipids, carotenoids, and fatty acid composition.* Biology, 2021. **10**(10): p. 1060. DOI: https://doi.org/10.3390/biology10101060.

[19] Wu, L.F., et al., *The feasibility of biodiesel production by microalgae using industrial wastewater.* Bioresource Technology, 2012. **113**: p. 14-18. DOI: https://doi.org/10.1016/j.biortech.2011.12.128.

[20] Amini Khoeyi, Z., J. Seyfabadi, and Z. Ramezanpour, *Effect of light intensity and photoperiod on biomass and fatty acid composition of the microalgae, Chlorella vulgaris.* Aquaculture International, 2012. **20**: p. 41-49. DOI: https://doi.org/10.1007/s10499-011-9440-1.

[21] Borella, L., et al., *Application of flashing blue-red LED to boost microalgae biomass productivity and energy efficiency in continuous photobioreactors.* Energy, 2022. **259**: p. 125087. DOI: https://doi.org/10.1016/j.energy.2022.125087.

[22] Krzemińska, I., et al., *Influence of photoperiods on the growth rate and biomass productivity of green microalgae.* Bioprocess and Biosystems engineering, 2014. **37**: p. 735-741. DOI: https://doi.org/10.1007/s00449-013-1044-x.

[23] Wong, Y., et al., *Effects of Light Intensity, Illumination Cycles on Microalgae Haematococcus Pluvialis for Production of Astaxanthin.* Illumination Cycles on Microalgae Haematococcus Pluvialis for Production of Astaxanthin, 2016: p. 1-6. DOI: https://doi.org/10.15436/2381-0750.16.1083.

[24] Yustinadiar, N., R. Manurung, and G. Suantika, *Enhanced biomass productivity of microalgae Nannochloropsis sp. in an airlift photobioreactor using low-frequency flashing light with blue LED.* Bioresources and Bioprocessing, 2020. **7**: p. 1-15. DOI: https://doi.org/10.1186/s40643-020-00331-9.

[25] Chong, C.C., et al., *Anaerobic digestate as a low-cost nutrient source for sustainable microalgae cultivation: A way forward through waste valorization approach.* Science of The Total Environment, 2022. **803**: p. 150070. DOI: https://doi.org/10.1016/j.scitotenv.2021.150070.

[26] Huang, X., et al., *Effects of nitrogen supplementation of the culture medium on the growth, total lipid content and fatty acid profiles of three microalgae (Tetraselmis subcordiformis, Nannochloropsis oculata and Pavlova viridis).* Journal of applied phycology, 2013. **25**: p. 129-137. DOI: https://doi.org/10.1007/s10811-012-9846-9.

[27] Zarrinmehr, M.J., et al., *Effect of nitrogen concentration on the growth rate and biochemical composition of the microalga, Isochrysis galbana.* The Egyptian Journal of Aquatic Research, 2020. **46**(2): p. 153-158. DOI: https://doi.org/10.1016/j.ejar.2019.11.003.

[28] Borah, D., et al., *An Integrated Approach for Simultaneous Monitoring and Data Acquisition on the Culture of Green Microalga Chlorella homosphaera Using Different LED Illumination.* BioEnergy Research, 2023. **16**(1): p. 601-610. DOI: https://doi.org/10.1007/s12155-022-10452-y.

[29] Markou, G., *Effect of various colors of light-emitting diodes (LEDs) on the biomass composition of Arthrospira platensis cultivated in semi-continuous mode.* Applied biochemistry and biotechnology 2014. **172**: p. 2758-2768. DOI: https://doi.org/10.1007/s12010-014-0727-3.

[30] Kim, S.H., et al., *Lipid and unsaturated fatty acid productions from three microalgae using nitrate and light-emitting diodes with complementary LED wavelength in a two-phase culture system.* Bioprocess and Biosystems engineering, 2019. **42**: p. 1517-1526. DOI: https://doi.org/10.1007/s00449-019-02149-y.

[31] Sirisuk, P., et al., *Effects of wavelength mixing ratio and photoperiod on microalgal biomass and lipid production in a two-phase culture system using LED illumination.*

Bioresource technology, 2018. **253**: p. 175-181. DOI: https://doi.org/10.1016/j.biortech.2018.01.020.

[32] López-Rosales, L., et al., *Modeling shear-sensitive dinoflagellate microalgae growth in bubble column photobioreactors.* Bioresource technology, 2017. **245**: p. 250-257. DOI: https://doi.org/10.1016/j.biortech.2017.08.161.

[33] Morales, M., L. Sánchez, and S. Revah, *The impact of environmental factors on carbon dioxide fixation by microalgae.* FEMS microbiology letters, 2018. **365**(3): p. fnx262. DOI: https://doi.org/10.1093/femsle/fnx262.

[34] Tan, X.-B., et al., *Nutrients recycling and biomass production from Chlorella pyrenoidosa culture using anaerobic food processing wastewater in a pilot-scale tubular photobioreactor.* Chemosphere, 2021. **270**: p. 129459. DOI: https://doi.org/10.1016/j.chemosphere.2020.129459.

[35] Bredda, E.H., et al., *Mixture design as a potential tool in modeling the effect of light wavelength on Dunaliella salina cultivation: an alternative solution to increase microalgae lipid productivity for biodiesel production.* Preparative Biochemistry and Biotechnology 2020. **50**(4): p. 379-389. DOI: https://doi.org/10.1080/10826068.2019.1697936.

CHAPTER 4C

To analyze the algal biomass and biofuel properties produced from the microalgae cultured in the developed PBR.

4C. To analyze the algal biomass and biofuel properties produced from the microalgae cultured in the developed PBR.

This chapter details the analytical findings to characterize the biomass and biofuels obtained from the microalgae culture systems developed during the current investigation. The calorific value, ash content, lipid content, GC-MS characterization, biofuel production estimation using ^{1}H-NMR spectroscopy, oil density, acid value, and carbon residue are characterized and compared with the global standards.

4C.1 Calorific value of Chlorella homosphaera biomass

The calorific value (CV) of the biomass obtained using pink and cool-white LED illuminations cultured in the STAMP system was investigated to determine the possibility of using the dried algal biomass as a direct combustion fuel. The CV of the dry microalgae biomass was found to be 12.74 ± 0.07 kJg^{-1} and 14.72 ± 0.04 kJg^{-1} for the cool-white and pink LED illuminate microalgae culture, respectively, as shown in Figure 4C.1. The CV obtained was in range of the CV reported by Chia et al. [1] who had reported to obtaining a CV of 13.76 kJg^{-1} for *Chlorella vulgaris* microalgae cultured under controlled conditions. The higher CV of the pink LED illuminated microalgae culture can be attributed to the higher oil content of the pink LED illuminated microalgae culture compared to the cool-white LED illuminated culture, as reported in the later section of this article.

After lipid extraction, the CV of the residual microalgae biomass was also investigated to determine its capability as a fuel source. The CV of the deoiled microalgae biomass of pink and cool-white illuminated microalgae was found to be 9.78±0.13 kJg^{-1} and 9.57±0.31 $kJg^{-1,}$ respectively. The CV obtained is in the range of rice husk, sawdust, and corn cob briquettes used for energy generation, having CVs of 8.74 kJg^{-1}, 9.91 kJg^{-1}, and 12.25 kJg^{-1}, respectively. Additionally, the CV obtained for the deoiled microalgae biomass is well for the deoiled microalgae biomass is well above the minimum standard CV range for heat generation, which is 6.27 kJg^{-1}– 6.98 kJg^{-1}, as reported by Awulu et al. [2]. Thus, it can be said that the microalgae biomass, as well as the deoiled microalgae biomass, has the potential to be used as a fuel source for energy generation.

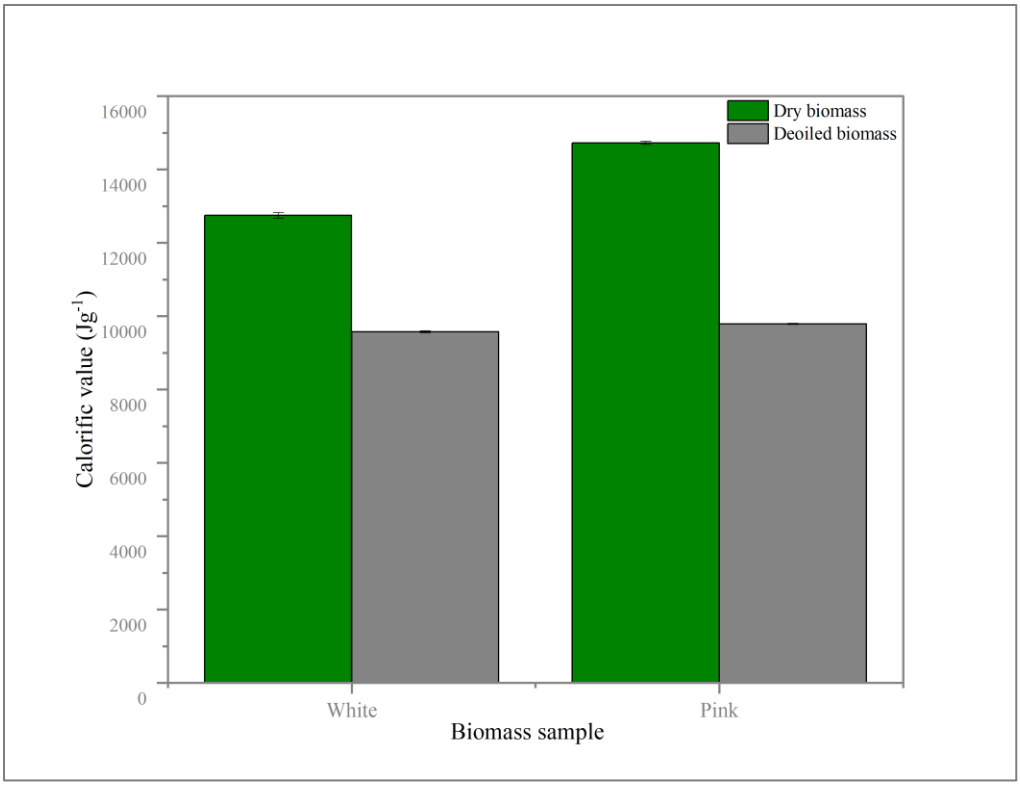

Figure 4C.1: Calorific value of dry microalgae biomass and deoiled microalgae biomass culture from the STAMP system using cool-white and pink LED illumination.

4C.2 Ash content of Chlorella homosphaera biomass

The microalgae biomass's ash content was evaluated, which is an important parameter reflecting its inorganic mineral composition. The ash content in microalgae biomass has positive and negative impacts depending on its final use. For instance, when using microalgae biomass for bioenergy applications, as in direct combustion, a high ash content in the biomass can lead to the formation of slag or ash deposition, degrading the performance, efficiency, and lifespan of the equipment [3, 4]. High ash content will also require additional ash removal pretreatment processes, increasing the cost of the derived biofuel [5, 6]. However, high ash content in microalgae biomass can benefit applications like animal feed or fertilizer production due to inorganic compounds like calcium, iron, magnesium, potassium, zinc, selenium, etc. [7-9]. Thus, the ash content in the microalgae biomass plays a significant role depending on the application.

The ash content obtained in the biomass cultured in the STAMP system was found to be 15.4± 0.51%, 18.5±0.68%, 14.23±0.52%, and 21.4±0.69% for dry biomass of cool-white LED illuminated, de-oiled biomass of cool-white LED illuminated, pink LED illuminated and deoiled

biomass of pink LED illuminated microalgae respectively, shown in Figure 4C.2. The obtained ash content values are a bit higher than the ash content of *Chlorella vulgaris* species obtained by Tokusoglu et al. [10], reporting 6.30 ± 0.02 % ash content, however, are in the range of ash content of *Isochrisis galbana* species having 16.08 ± 0.03% ash content. The high ash content can be attributed to several factors, one being the harvesting method used. The chemical flocculation method we implemented during the investigation resulted in a higher ash content than centrifugation harvesting, which was implemented by Tokusoglu et al. in their investigation [10]. Wang et al. [11], has highlighted the influence of harvesting technique on the ash content of the microalgae biomass, with ash content varying from 10.22 ± 0.30% to 14.69 ± 0.02% in the *Scenedesmus obliquus* microalgae harvested using centrifugation and flocculation respectively. Thus, depending on the end use, the harvesting needs to be optimized as it plays a significant role in the ash content of the final biomass.

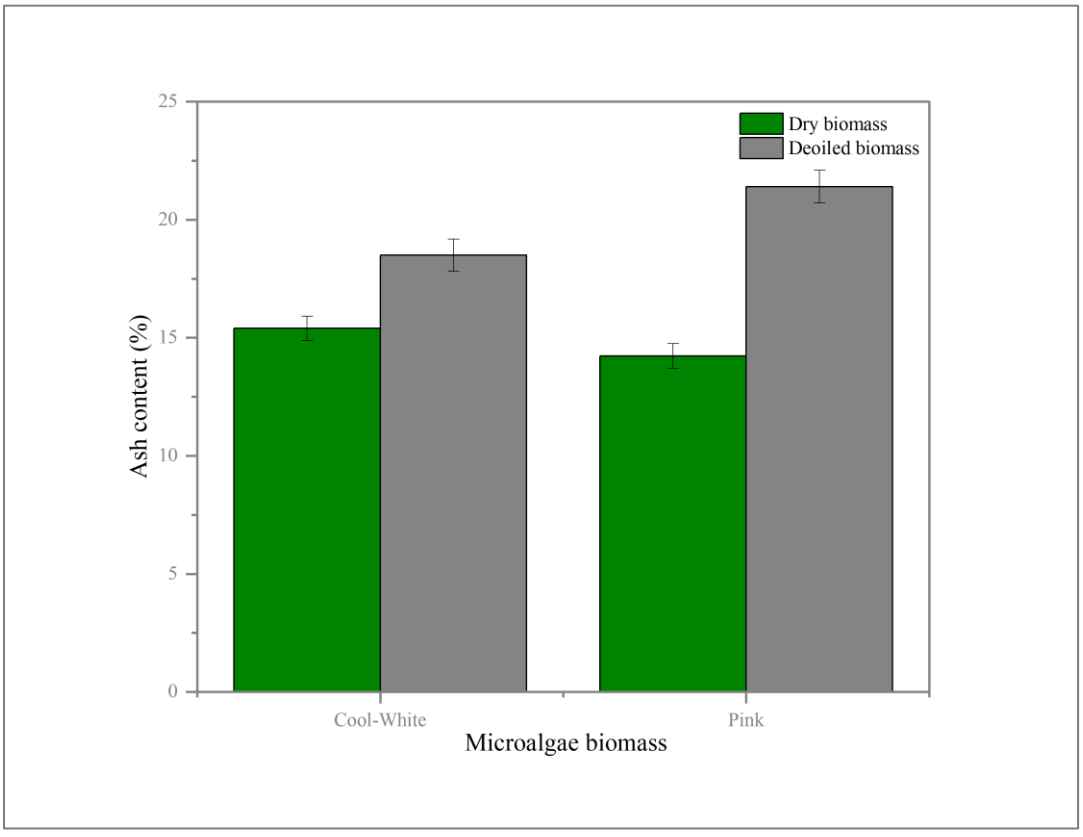

Figure 4C.2: Ash content of dry microalgae biomass and deoiled microalgae biomass culture from the STAMP system using cool-white and pink LED illumination.

4C.3 Lipid analysis of *Chlorella homosphaera* biomass

The lipid content of the *Chlorella homosphaera* microalgae cultivated in the STAMP using cool-white and pink LEDs was evaluated. Cool-white and pink LED illumination yielded 9.5±0.35 % and 17.7±0.4 % lipid content while growing in the STAMP system. The lipid content in microalgae species depends on factors like nitrogen, light wavelength, light duration, light intensity, and airflow, as described in the previous chapter. Apart from the above factors, there are many other factors affecting the lipid content in a microalgae species, like salinity, light stress, temperature, and pH, which need to be studied and optimized later to achieve higher lipid productivity. The acid values of the microlage lipid were found to be 22.42 and 36.70 mg KOH/g resulting in a fame content of 11.26 and 18.44 % for the cool-white and pink LED illuminated microlage species respectively. Ratromski et al. [12] reported a variation of lipid content in *Chlorella vulgaris* microalgae species from 5.75% to 11.81% depending on the nutrient stress applied. Similarly, Converti et al. [13] reported a 5.9% to 16.41% variation, almost in the range obtained in our case, depending on temperature and nitrogen concentration variation. Thus, lipid content in microalgae is a complex process that depends on multitudes of factors, and additional studies will be needed to achieve the desired values.

4C.4 Lipid characterization of *Chlorella homosphaera* microalgae using GCMS

The lipid composition significantly influences the characteristics of the biodiesel produced from it due to physiochemical characteristic differences of different components present in the lipid. For instance, the presence of a high proportion of saturated and monosaturated fatty acid is desired in biodiesel as it increases the cetane number of the biodiesel, produces lesser NOx during combustion, and makes it desirable for storage due to a lesser tendency towards oxidation [14]. However, saturated fatty acid leads to a high pour point, making it undesirable for use in cold environments. On the other hand, a higher concentration of unsaturated fatty acid decreases the pour point of the biodiesel, making it suitable for cold environments. However, due to its high affinity toward oxidation, it is undesirable for storage.

The the lipid composition of the *C. homosphaera* analysed using GCMS is presented in Table 4C.1. However, in both the cases Palmatic acid and Oleic acid are found to be predominantly present, which enhances the possibility of using the biodiesel produced ftom these lipids to be

suitable for engine applications [15]. High content of Oleic acid and Palmatic acid in the lipid composriotion of *Chlorella* microlage lipid are also reported by Aguro et al. [16]. From the acid composition it can be stated that factors like illumination type significantly influences the fatty acid composition. A detailed investigation regarding the effect of fatty acid composition and its optimization can be kept as part of future research prospects.

Table 4C.1: Composition of the *C homosphaera* microalgae lipid analysed using GCMS.

Fatty Acid	Composition (%)	
	Cool-White LED	Pink LED
Trideconeoic acid	1.22	0.8
Myristic acid	1.7	1.9
Myristoleic acid	3.2	3.4
Palmitic acid	34.4	42.2
Stearic acid	2.8	4.6
Oleic acid	21.2	19.4
Linoleic acid	5.4	4.7
Linolenic acid	2.4	1.7
Arachidic acid	1.9	2.4
Octadecanoic acid	2.4	1.2

4C.5 ^{1}H NMR analysis of *C homosphaera* lipid and biodiesel

The microalgae lipid obtained from the STAMP system, cultured using pink LED illumination, was processed into biodiesel via a transesterification reaction. Pink LED-based lipid was selected for further processing owing to the high productivity achieved in the current setup. The obtained lipid and the biodiesel or FAME (fatty acid methyl ester) derived from the lipid were confirmed using ^{1}H NMR, also known as proton nuclear magnetic resonance spectroscopy. ^{1}H NMR is the application of nuclear magnetic resonance in NMR spectroscopy with respect to hydrogen-1 nuclei within the molecule of a substance to determine the structure of the molecule [17]. In simple words, ^{1}H NMR spectra tell us how many C and H atoms are in a molecule and which atoms are attached to which [18].

In the current study, the picks appeared in the 4.0-5.0 ppm region of the ^{1}H NMR spectra of *C homosphaera* lipid, Figure 4C.3(a), indicates glyceridic protons, which confirms the presence of triglycerides in the lipid sample, which disappears upon transesterification of the microalgae lipid, as can be seen in the ^{1}H NMR of the biodiesel sample in Figure 4C.3(b). The sharp peaks in the 3.6 ppm region and the peak at 2.3 ppm in the biodiesel sample in Figure 4C.3(b) represent methyl ester moiety protons and α-carbonyl methylene groups, respectively, confirming the formation of biodiesel. Further physiochemical characterization of the biodiesel is presented in the following section. Based on the ^{1}H NMR spectra, biodiesel conversion percentage was calculated from the integral values of the methoxy proton (~3.6 ppm) and α-methylene proton peaks (~2.3 ppm) and was found to be 90.6% which is reasonable. However, there are scope for further improvement of the conversion percentage by optimization of the reaction parameters, which can be done in future studies.

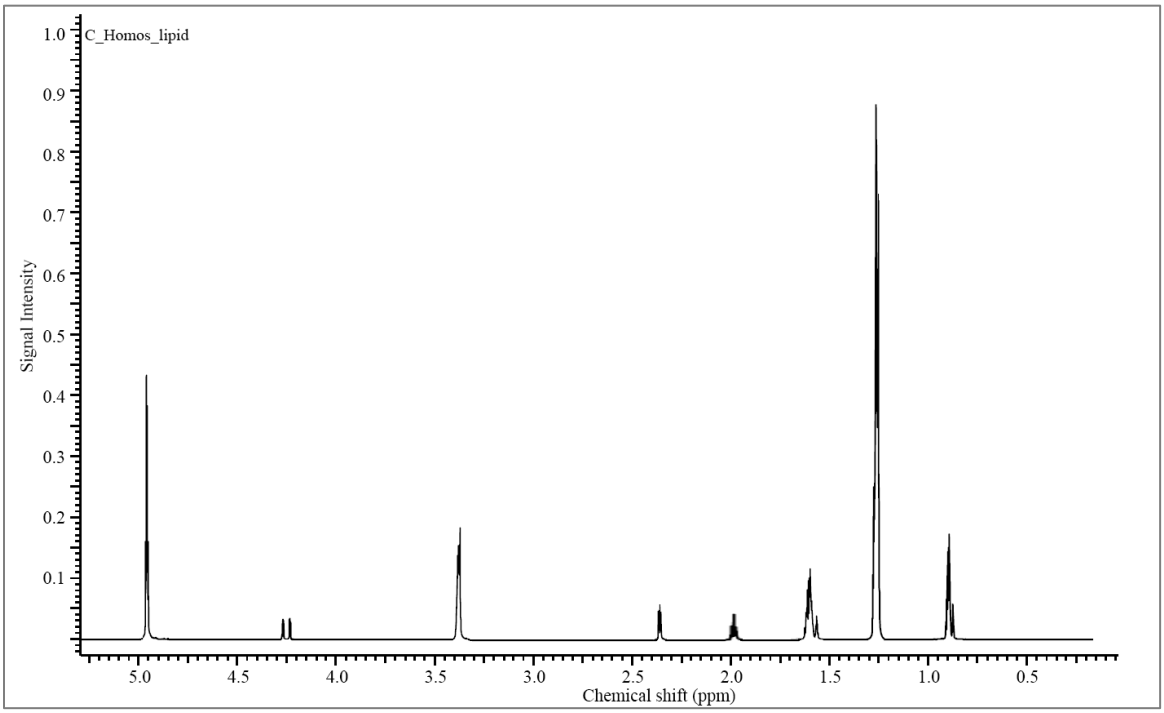

Figure 4C.3 (a): ^{1}H NMR spectra of *C homosphaera* microalgae lipid cultured with pink LED illumination in the STAMP system.

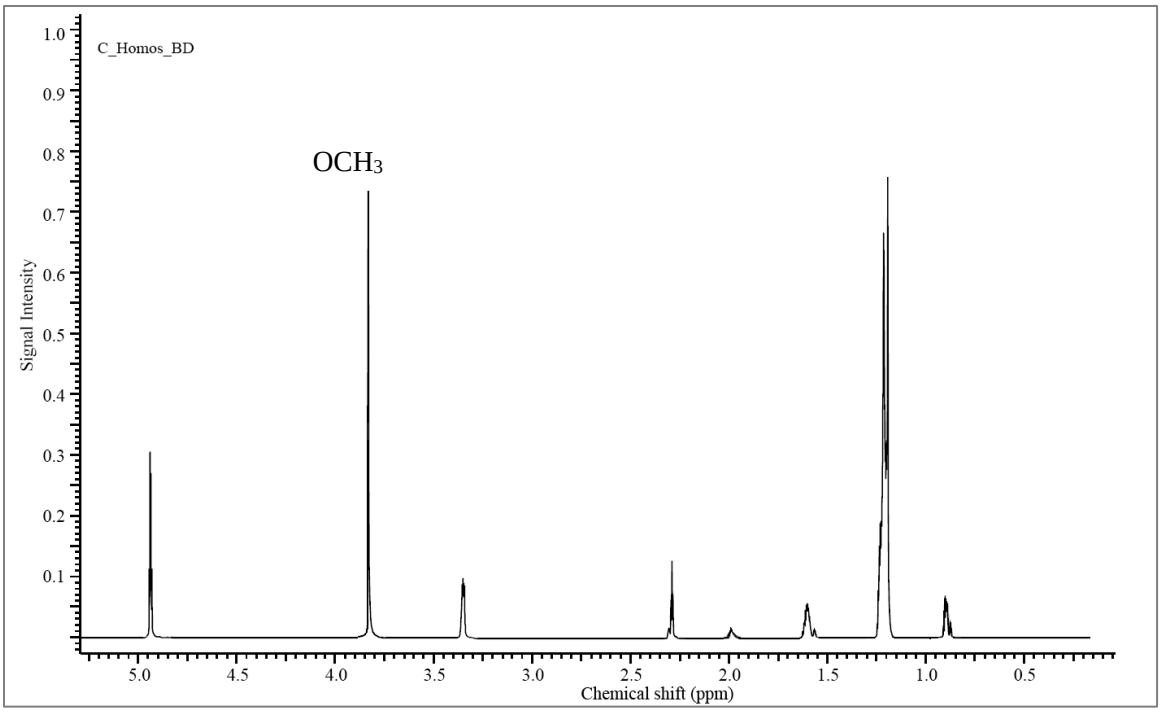

Figure 4C.3 (b): ^{1}H NMR spectra of *C homosphaera* microalgae biodiesel derived from the pink LED illumination microalgae cultured in the STAMP system.

4C.6 Characterization of fuel properties of the derived biodiesel

The biodiesel synthesized from the pink LED illuminated culture of *C homosphaera* cultured in the STAMP system was analyzed for its fuel properties. The calorific value of the obtained biodiesel was found to be 36.84 MJ $kg^{-1,}$ which is slightly lesser than the desired value of around 39.07 MJ kg^{-1} obtained from palm biodiesel, as reported by Balfas et al. [19]. The CV of biodiesel is generally lower due to higher oxygen content in it as compared to petroleum diesel [20], and the obtained biodiesel, thus, has scope for further improvement by altering the composition of the fuel using different light or other stress conditions.

The other fuel properties like carbon residue, acid value, density, and kinematic viscosity obtained for the biodiesel synthesized form pink LED illuminated culture of *C homosphaera* microalgae are presented in Table 4C.2, are primarily in accordance with the ASTM (American Society for Testing and Materials) and the EN (European Standard).

There is further scope for improvement with further development of the STAMP system and with further improvement in the culture conditions, such as introducing stress conditions, incorporation of other microalgae strains, etc., discussed in the following chapter.

Table 4C.2: Characterization of the biodiesel derived from pink illuminated *C homosphaera* microalgae cultivated in the STAMP

Property	C.H_B.D.	Desired value	Reference
Calorific value (MJ kg^{-1})	36.84	39.07	[19]
Carbon residue (% wt.)	0.01	0.3 (max)	EN14214
Acid value (mg KOH g^{-1})	0.11	0.5	ASTM D6751
Density (kg m^{-3} at 15 °C)	892	860-900	EN14214
Kinematic Viscosity ($mm^2 s^{-1}$, at 40 °C)	3.6	1.9-6.0	ASTM D6751

C.H_B.D: Chlorella homosphaera biodiesel

4C.7 Summary

The chapter analyzes the biomass, lipid, and synthesized biodiesel from *C homosphaera* microalgae cultivated in the STAMP system. The biomass obtained demonstrated CV up to 14.72 ± 0.04 kJg^{-1}, which is suitable to be used as a solid fuel for heat generation. The fuel properties for synthesized biodiesel, like the calorific value of 36.84 MJ kg^{-1}, carbon residue of 0.01%, acid value of 0.11 mg KOH g^{-1}, density of 892 kg m^{-3} at 15 ℃, and kinematic viscosity of 3.6 mm^2s^{-1} at 40 ℃ promising and have scope for further improvements.

References

[1] Chia, M.A., A.T. Lombardi, and M.d.G. Gama Melao, *Calorific values of C hlorella vulgaris (T rebouxiophyceae) as a function of different phosphorus concentrations.* Phycological Research, 2013. **61**(4): p. 286-291. DOI: https://doi.org/10.1111/pre.12026.

[2] Awulu, J., P.A. Omale, and J. Ameh, *Comparative analysis of calorific values of selected agricultural wastes.* Nigerian Journal of Technology, 2018. **37**(4): p. 1141-1146. DOI: https://doi.org/10.4314/njt.v37i4.38.

[3] Hossain, N. and N.A.H. Morni, *Co-pelletization of microalgae-sewage sludge blend with sub-bituminous coal as solid fuel feedstock.* BioEnergy research, 2020. **13**(2): p. 618-629. DOI: https://doi.org/10.1007/s12155-019-10061-2.

[4] Vassilev, S.V. and C.G. Vassileva, *Composition, properties and challenges of algae biomass for biofuel application: An overview.* Fuel, 2016. **181**: p. 1-33. DOI: https://doi.org/10.1016/j.fuel.2016.04.106.

[5] Mata, T.M., A.A. Martins, and N.S. Caetano, *Microalgae for biodiesel production and other applications: a review.* Renewable and sustainable energy reviews, 2010. **14**(1): p. 217-232. DOI: https://doi.org/10.1016/j.rser.2009.07.020.

[6] Onumaegbu, C., et al., *Pre-treatment methods for production of biofuel from microalgae biomass.* Renewable and sustainable energy reviews, 2018. **93**: p. 16-26. DOI: https://doi.org/10.1016/j.rser.2018.04.015.

[7] Fabregas, J. and C. Herrero, *Marine microalgae as a potential source of minerals in fish diets.* Aquaculture 1986. **51**(3-4): p. 237-243. DOI: https://doi.org/10.1016/0044-8486(86)90315-7.

[8] Silva, M., et al., *Microalgae as potential sources of bioactive compounds for functional foods and pharmaceuticals.* Applied Sciences, 2022. **12**(12): p. 5877. DOI: https://doi.org/10.3390/app12125877.

[9] Saha, S.K., et al., *Microalgae as a source of nutraceuticals.* Phycotoxins: chemistry and biochemistry, 2015: p. 255-291. DOI: https://doi.org/10.1002/9781118500354.ch12.

[10] Tokuşoglu, Ö. and M. Üunal, *Biomass nutrient profiles of three microalgae: Spirulina platensis, Chlorella vulgaris, and Isochrisis galbana.* Journal of food science, 2003. **68**(4): p. 1144-1148. DOI: https://doi.org/10.1111/j.1365-2621.2003.tb09615.x.

[11] Wang, S., et al., *Microalgae harvest influences the energy recovery: a case study on chemical flocculation of Scenedesmus obliquus for biodiesel and crude bio-oil production.* Bioresource technology, 2019. **286**: p. 121371. DOI: https://doi.org/10.1016/j.biortech.2019.121371.

[12] Ratomski, P. and M. Hawrot-Paw, *Influence of nutrient-stress conditions on Chlorella vulgaris biomass production and lipid content.* Catalysts, 2021. **11**(5): p. 573. DOI: https://doi.org/10.3390/catal11050573.

[13] Converti, A., et al., *Effect of temperature and nitrogen concentration on the growth and lipid content of Nannochloropsis oculata and Chlorella vulgaris for biodiesel production.* Chemical Engineering and Processing: Process Intensification, 2009. **48**(6): p. 1146-1151. DOI: https://doi.org/10.1016/j.cep.2009.03.006.

[14] Van Gerpen, J. *Cetane number testing of biodiesel*. in *Proceedings, third liquid fuel conference: liquid fuel and industrial products from renewable resources*. 1996. American Society of Agricultural Engineers St. Joseph, MI.

[15] Behera, B., B. Dey, and P. Balasubramanian, *Algal biodiesel production with engineered biochar as a heterogeneous solid acid catalyst.* Bioresource technology, 2020. **310**: p. 123392. DOI: https://doi.org/10.1016/j.biortech.2020.123392.

[16] Aguoru, C. and P. Okibe, *Content and composition of lipid produced by Chlorella vulgaris for biodiesel production.* Advances in life science and technology, 2015. **36**: p. 96-100.

[17] Nikolić, V., et al., *Administration routes for nano drugs and characterization of nano drug loading*, in *Characterization and biology of nanomaterials for drug delivery*. 2019, Elsevier. p. 587-625.

[18] Jacobsen, N.E., *NMR spectroscopy explained: simplified theory, applications and examples for organic chemistry and structural biology*. 2007: John Wiley & Sons.

[19] Balfas, R.N., et al., *Characteristics of Biodiesel Produced from Crude Palm Oil through Non-Alcohol Synthesis Route Using Dimethyl Carbonate and Immobilized Eco-Enzyme Catalyst.* Energies, 2024. **17**(7): p. 1551. DOI: https://doi.org/10.3390/en17071551.

[20] Kaisan, M., et al., *Calorific value, flash point and cetane number of biodiesel from cotton, jatropha and neem binary and multi-blends with diesel.* Biofuels-state of development, 2017. DOI: https://doi.org/10.1080/17597269.2017.1358944.